

Masonry Walls under Shear Test: a CM Modeling

E. Ferretti¹, E. Casadio and A. Di Leo¹

Abstract: In this study, the Cell Method (CM) is applied in order to investigate the failure mechanisms of masonry walls under shear force. The direction of propagation is computed step-wise by the code, and the domain is updated by means of a propagation technique of intra-element nodal relaxation with re-meshing. The crack extension condition is studied in the Mohr/Coulomb plane, using the criterion of Leon. The main advantage of using the CM for numerical analyses of masonry is that the mortar, the bricks and the interfaces between mortar and bricks can be modeled without any need to use homogenization techniques, simply providing each of them with their own constitutive properties. The capability of the CM to handle domains with more than one material is exploited to capture how the propagation direction changes when the crack overcome the joints or passes from the brick to the interface and to the mortar. Also, the principal stresses and principal directions of stress are mapped for the bricks, the interfaces and the mortar. In comparison with those presented in Ferretti (2003) and Ferretti (2004a), the computational capabilities of the CM code have been improved considerably. Actually, a new version of the CM code has been implemented, which is able to self-compute the position of crack initiation and manage several cracks propagating at the same time. This allows us not to impose the number and the position of crack initiations a-priori, letting the code estimate them as the imposed displacement is increased. Interactions between propagating cracks are simply taken into account by the code, leading to modification of the failure direction or to crack arrest as soon as a new crack activates. The code is also able to self-estimate whether or not one or

more cracks bifurcate and to follow the propagation of each branch of bifurcation.

Keyword: Cell Method, Adaptive Re-Meshing, Masonry, Shear Test, Crack Initiation, Multiple Crack Propagation, Crack Path, Crack Bifurcation.

1 Masonry modeling

Masonry is a heterogeneous material obtained by regular arrangement of bricks and mortar. In a broad sense, then, masonry may be considered as a periodic composite continuum.

Numerous models have been proposed in literature, in order to study the mechanical behavior of masonry. Nevertheless, a general approach, able to predict the ultimate load bearing capacity of masonry under in- and out-of-plane loads, is still far for being proposed. The difficulty in modeling masonry structures depends on many causes. The two most important ones are the heterogeneous character of masonry and the brittle behavior of joints.

At present, the numerical models for studying masonry are based on three different approaches:

Micro-modeling. The masonry is modeled as a two-phase medium (Fig. 1), with bricks and mortar joints being taken into account distinctly as separate units [Lofti and Benson Shing (1994), Lourenço and Rots (1997), Gambarotta and Lagomarsino (1997, Part I and Part II), Ferris and Tin-Loi (2001), Giambanco Rizzo and Spallino (2001), Formica Sansalone and Casciaro (2002), etc.].

This approach allows a point-to-point prediction of the stress and strain fields, but its applicability is limited to the structural analysis of small panels. In some cases, reasonable simplifications have been introduced, in order to extend

¹ DISTART, Scienza delle Costruzioni, Facoltà di Ingegneria, Alma Mater Studiorum, Università di Bologna, Viale Risorgimento 2, 40136 (BO), ITALY.

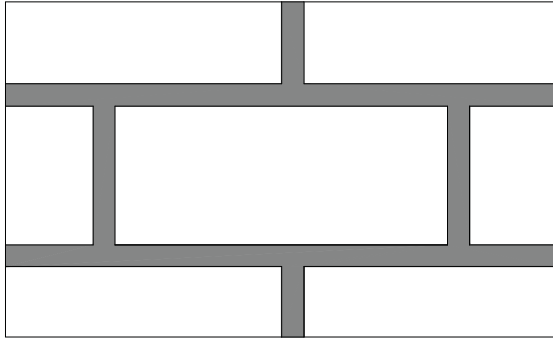


Figure 1: Basic cell for micro-modeling

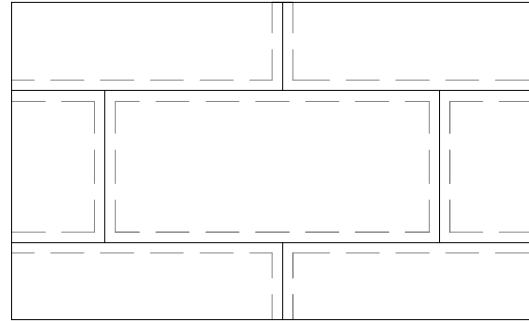


Figure 2: Basic cell for simplified micro-modeling

the method to complex walls belonging to existing real buildings, such as using zero-thickness interfaces for the joints [Lofti and Shing (1994), Lourenço and Rots (1997)].

Simplified micro-modeling: homogenization techniques. The masonry is modeled as a homogeneous medium, equivalent to a strongly heterogeneous one as far as the geometry and property of the constituent materials are concerned. The homogenization theory for periodic heterogeneous media [Carvelli Maier and Taliercio (2000)] allows the global behavior of masonry to be derived from the behavior of the constitutive materials [Kralj Pande and Middleton (1991), Maier Nappi and Papa (1991), Shrive and England (1991), Pietruszczak and Niu (1992), Alpa and Monetto (1994), de Felice (1995), Masiani Rizzi and Trovalusci (1995), Lourenço (1996), Lee Pande and Kralj (1998), Cecchi and Di Marco (2000)]. The method identifies an elementary cell (Fig. 2), which generates all the panel by regular repetition. The core of the method is the formulation of a differential problem based on the single cell. The solution of such a problem leads to the definition of homogenized constitutive relations, which work as macroscopic descriptors for the behavior of the heterogeneous body.

Complete and technical presentations of the homogenization theory, based on asymptotic analysis, may be found in Bensoussan Lions and Papanicolaou (1978), Duvaut (1984) and Sanchez-Palencia (1980).

The homogenization techniques have been em-

ployed extensively for modeling masonry structures in the elastic field: for the elastic linear field, see Pande Liang and Middleton (1989), Anthoine (1995), Cecchi and Rizzi (2001), Cecchi and Sab (2002), Cecchi Milani and Tralli (2004); for the elastic non-linear field, see Zucchini and Lourenço (2002). For the inelastic range, Luciano and Sacco (1997) proposed a brittle damaging model with a unit cell composed of bricks, mortar and a finite number of fractures on the interfaces, Massart (2003) and Pegon and Anthoine (1997) used a finite element approach assuming either elastic-plastic or damaging constitutive laws for bricks and mortar, De Buhan and de Felice (1997) proposed a homogenized limit analysis of masonry with a pure Mohr Coulomb failure criterion, where the bricks are supposed to be infinitely resistant and the joint interfaces to be of zero thickness. The limit analysis combined with homogenization techniques is able to reproduce the anisotropy at collapse and the scarce tensile strength, requiring only a reduced number of mechanical parameters of the constituent materials. Once the homogenized strength domain for masonry is available, the limit analysis can be applied easily to entire panels.

Macro-modeling. The goal of this approach is large-scale structural calculation. To this end, the masonry is modeled as a homogeneous medium (Fig. 3), by means of the definition of a fictitious continuous material and yield surfaces extracted by fitting technique of experimental results [Lourenço de Borst and Rots (1997)].

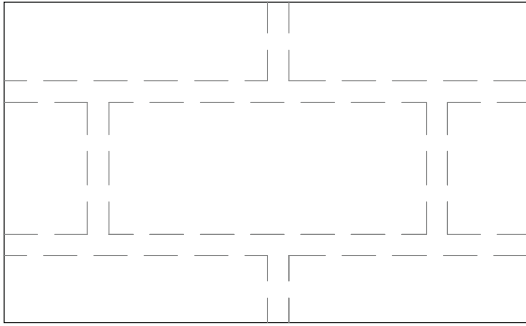


Figure 3: Basic cell for macro-modeling

Usually, the mechanical properties required by the model are derived from experimental data, with the consequence that the results are limited to the conditions under which the data are obtained. Thus, these models must be calibrated over the single test and are not generalizable.

One of the most widely adopted macro-modeling approaches models masonry as a no tension material (NTM) [Heyman (1966), Romano and Romano (1979), Como and Grimaldi (1985), Giacquinta and Giusti (1985), Romano and Sacco (1987), Del Piero (1989), Di Pasquale (1992), Del Piero (1998)]. According to this approach, the masonry is schematized as a homogeneous elastic material which cannot support tensile stress. This formulation is very attractive because of the simplicity of the mechanical assumptions, but does not seem able to lead to robust numerical tools [Milani (2004)]. The main reason for this is that the constitutive equations for masonry are generally non associated, both for taking into account the role played by the friction between the bricks in determining the strength in masonry panels subjected to horizontal actions, and avoiding the positive principal stresses, not admissible for an NTM, provided by an associate flow rule when a plane stress state with shear stress and vertical compressive pressure is assumed.

Several other models of macro-modeling can be found in the technical literature, some of which [Lourenço (1995), Berto Saetta Scotta and Vitaliani (2002)] were developed in order to take into account some distinctive aspects of masonry, such

as anisotropy in the elastic range and the post-peak softening behavior.

Another possible classification of the models for masonry analysis is the one that distinguishes between discrete and continuum models [Luciano and Sacco (1998)]. The discrete models are used to analyze superimposed blocks, schematized as linear elastic, while the interfaces are modeled using the unilateral Coulomb friction law [Chiostrini and Vignoli (1989), Grimaldi Luciano and Sacco (1992)]. Micro-modeling with zero-thickness interfaces for the joints is an example of discrete model.

The continuum models may use both phenomenological and micromechanical constitutive laws for the masonry. When a phenomenological law is used, the constitutive response of the masonry must be determined by experimental tests. This is the case of the macro-modeling and, in particular, of the NTM phenomenological continuous law. The micromechanical analysis, on the contrary, models the masonry as a heterogeneous material, made of bricks in a matrix of mortar. This is the case of the micro-modeling and the simplified micro-modeling, when a homogenization technique based on micromechanical models of the periodic structure [Aboudi (1990), Mura (1987)] is added to the micromechanical analysis.

2 General remarks on the Cell Method (CM)

With the aim of framing the CM [Tonti (2001a)], a Finite Formulation Technique, into the traditional approaches used for modeling masonry (Section 1), we could say that the CM allows us to build a continuum model which lies at the level of the micro-modeling, affording a high degree of detail in the analysis.

As far as the main characteristics of the CM are concerned, we will only recall here that the stress field is evaluated on the dual elements (blue elements in Fig. 4) of a Delaunay triangulation (red elements in Fig. 4), by means of a discrete analysis, and that the method allows us to treat domains easily with several materials (Fig. 5). For a complete discussion on the advantages connected to the Discrete Formulation, see Ferretti (2005).

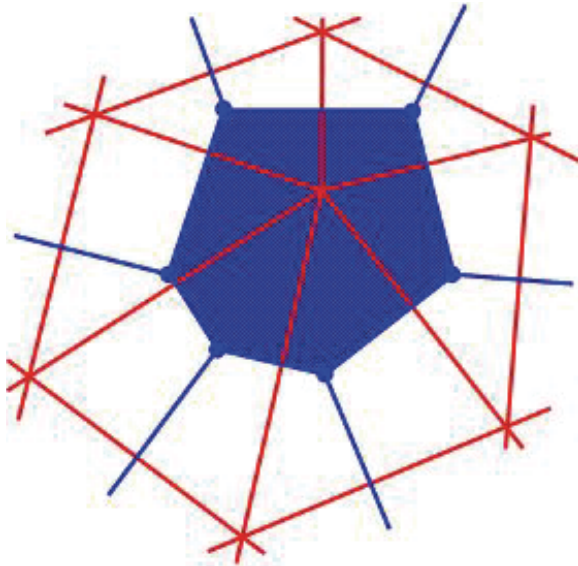


Figure 4: Mesh of Delaunay/Voronoi

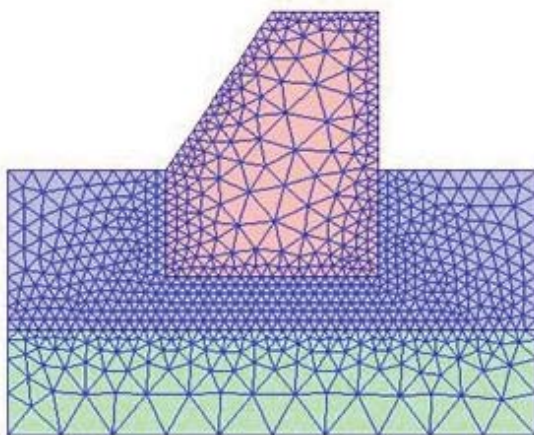


Figure 5: Example of modeling on domain made up of several materials: each color represents a different material

Since it performs a discrete analysis, the CM has often been compared to the direct or physical approach initially used in the Finite Elements Method (FEM). Nevertheless, it must be said that in the direct or physical approach, the discrete formulation is induced by the differential formulation, which represents an intermediate step with limit process and field variables associated to points, well described by means of systems of coordinates (Fig. 6). The discrete formulation is then obtained using the two theorems of

Gauss and Stokes. The Finite Volume Method (FVM) and the Finite Differences Method (FDM) are also based on a differential formulation. In the CM, on the contrary, only discrete operators are used and the cell complexes replace the coordinate systems for describing not only points, but also lines, surfaces, and volumes (Fig. 6). 0- and more than 0-dimensional variables are described directly, avoiding the limit process and the subsequent reduction of the global variables to point variables, by associating them with nodes, edges, surfaces, and volumes of the cell complexes. The governing equations are expressed in the discrete form directly.

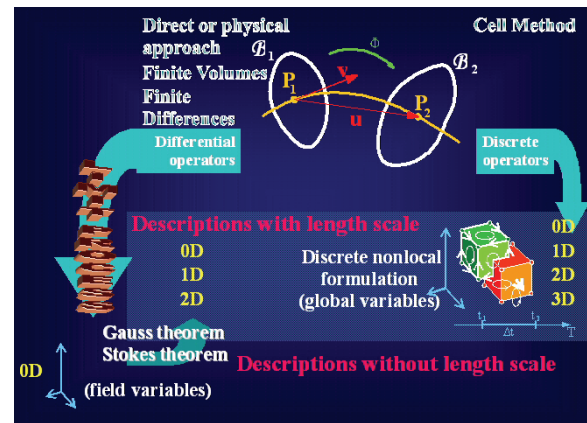


Figure 6: How to achieve the solution through the Cell Method and the differential formulation in the mechanics of solids

The geometrical structure of space is very rich with the CM. It is possible, for example, to define an inner orientation for the elements in dimension 0, 1, 2 and 3 (see the inner orientation for the green elements in Fig. 6). These oriented elements define the first cell complex. Then, by considering the planes which are equidistant from the nodes of the first cell complex, we can define a second cell complex (the elements of which are the orange ones in Fig. 6), which turns out to be provided with an outer orientation.

CM has been applied to different fields of physics science and engineering, such as acoustics [Tonti (2001b)], electrostatics [Bettini and Trevisan (2003)], magnetostatics [Trevisan and Kettunen (2004)], Eddy currents [Specogna and Trevisan

(2005)], electromagnetics in the time-domain [Marrone and Mitra (2004)] and in the frequency-domain [Marrone Grassi and Mitra (2004)], fracture mechanics [Ferretti (2003), Ferretti (2004a), Ferretti (2004c), Ferretti and Di Leo (2003)], elastodynamics [Cosmi (2005)] and fluid dynamics [Straface Troisi and Gagliardi (2006)]. The CM has been also applied to problems of thermal conduction, diffusion, biomechanics, heterogeneous materials modeling, mechanics of porous materials and structural mechanics. Recently, Heshmatzadeh and Bridges (2007) have compared in detail CM and FEM in electrostatics, proving the equivalence of the coefficient matrices for a Voronoi dual mesh and linear shape functions in the FEM, also showing that the use of linear shape functions in FEM is equivalent to the use of a barycentric dual mesh for charge vectors.

As discussed in Ferretti (2005), the main difference between the differential and the discrete approaches concerns the nonlocal description of the continuum. The different description of nonlocality comes from performing (differential approach) or not performing (discrete approach) the limit process. In the first case, the global variables are reduced to point (and instant) variables, causing the loss of metrics. Consequently, metrics must be reintroduced a-posteriori, by means of a length scale, if we want to describe the nonlocal effects. Usually, the length scale is introduced into the material description, leading to nonlocal constitutive relationships. In the second case, on the contrary, we do not need to recover the length scale, since the limit process is avoided and the length scale is preserved in the governing equations. Thus, the CM allows us to obtain a nonlocal formulation by using local constitutive laws and discrete operators.

3 CM analysis for self-weight of a masonry wall

As said above (Section 2), the CM manages domains made of several materials very easily, allowing a micro-modeling approach. The constitutive laws we used for mortar and bricks are shown in Figs. 7 and 8, respectively.

The monotonic non-decreasing law used for the

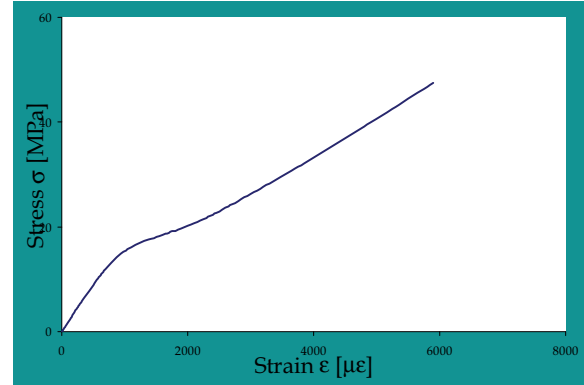


Figure 7: Constitutive law adopted for the mortar

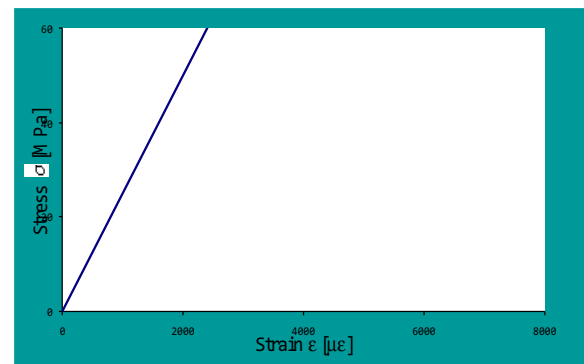


Figure 8: Constitutive law adopted for the bricks

mortar is an effective law, analogous to that derived for concrete, by means of the procedure of the effective law [Ferretti (2001); Ferretti and Di Leo (2003); Ferretti (2004b)]. The procedure of the effective law is a new experimental procedure for identifying the constitutive law in uniaxial compression for brittle heterogeneous materials. This procedure produces evidence against the existence of strain-softening (i.e. the decline of stress at increasing strain) and identifies a monotone strictly nondecreasing material law for concrete specimens in uniaxial compression (Fig. 10), having average stress versus average strain diagrams, $\bar{\sigma} - \bar{\epsilon}$, which are softening (Fig. 9).

The high degree of detail allowed by the CM can be appreciated on the stress analysis for self-weight, performed for the masonry wall in Fig. 11. The cell-to-cell map of the stress along the y axis (Fig. 12a and detail in Fig. 12b) shows

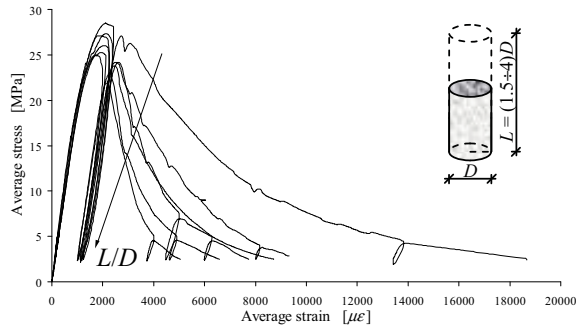


Figure 9: Size and softening effect for the $\bar{\sigma} - \bar{\epsilon}$ laws

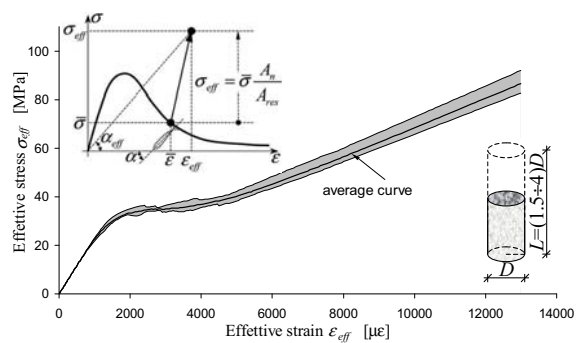


Figure 10: Dispersion range of the effective law for variable slenderness and average curve

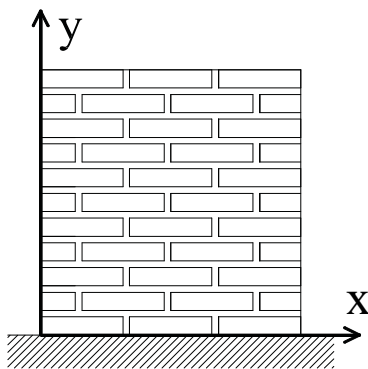


Figure 11: Scheme of the wall for self-weight analysis

an effect of negative friction on the vertical joints. Actually, due to the difference between the stiffness of the two materials, the mortar gets hold of the bricks, which are more stressed just near the vertical joints. The mortar, on the contrary, unloads near the vertical joints and this unloading

also involves the brick below. The principal directions of stress are plotted in Fig. 12c, which shows another interesting phenomenon: the rotation of the principal directions of stress at the intersection between vertical and horizontal joints.

As far as the isolines of stress are concerned, we can see that they are strongly influenced by the masonry lay-up, in the sense that they follow the interfaces between mortar and bricks. The isolines for the first and the second principal stress are shown in figs. 13 and 14, respectively. Since the masonry wall is subjected only to its own weight, the two principal stresses are quite similar to the stresses along the x and y axes. In particular, the second principal stress coincides with the stress along the x axis. Moreover, from the three-dimensional surface of the second principal stress (Fig. 15) we can see once more how the stress field is influenced by the mortar lay-up, with the mortar being more stressed than the bricks on the horizontal joints and less stressed on the vertical joints. The neutral plane in Fig. 15 (the plane $\sigma_x = 0$) shows a sort of arch effect of the stress, due to the constraint on the base, with compression stresses near the base of the wall and weak tensile stresses on the upper part of the wall.

Near the neutral axis (the line of intersection between the neutral plane and the three-dimensional surface in Fig. 15), the stresses in the mortar and the bricks have opposite sign: tension for bricks (red arrows in Fig. 16) and compression for the mortar (blue arrows in Fig. 16).

On the basis of this analysis, we can say that the presence of the mortar is disadvantageous for the masonry, in the sense that it is the bricks which confine the mortar, and not the contrary, due to the higher stiffness of bricks in comparison to the stiffness of the mortar. The stress also changes sign inside the bricks near the neutral axis (Fig. 17), with compression stresses on the middle of the brick, which corresponds to the intersections between vertical and horizontal joints. Once more, the change of stress sign depends on the difference between the two stiffnesses.

The behavior of the tensile state of stress is more emphasized by the frontal view of the stress surface (Fig. 18), showing a weak tensile stress for

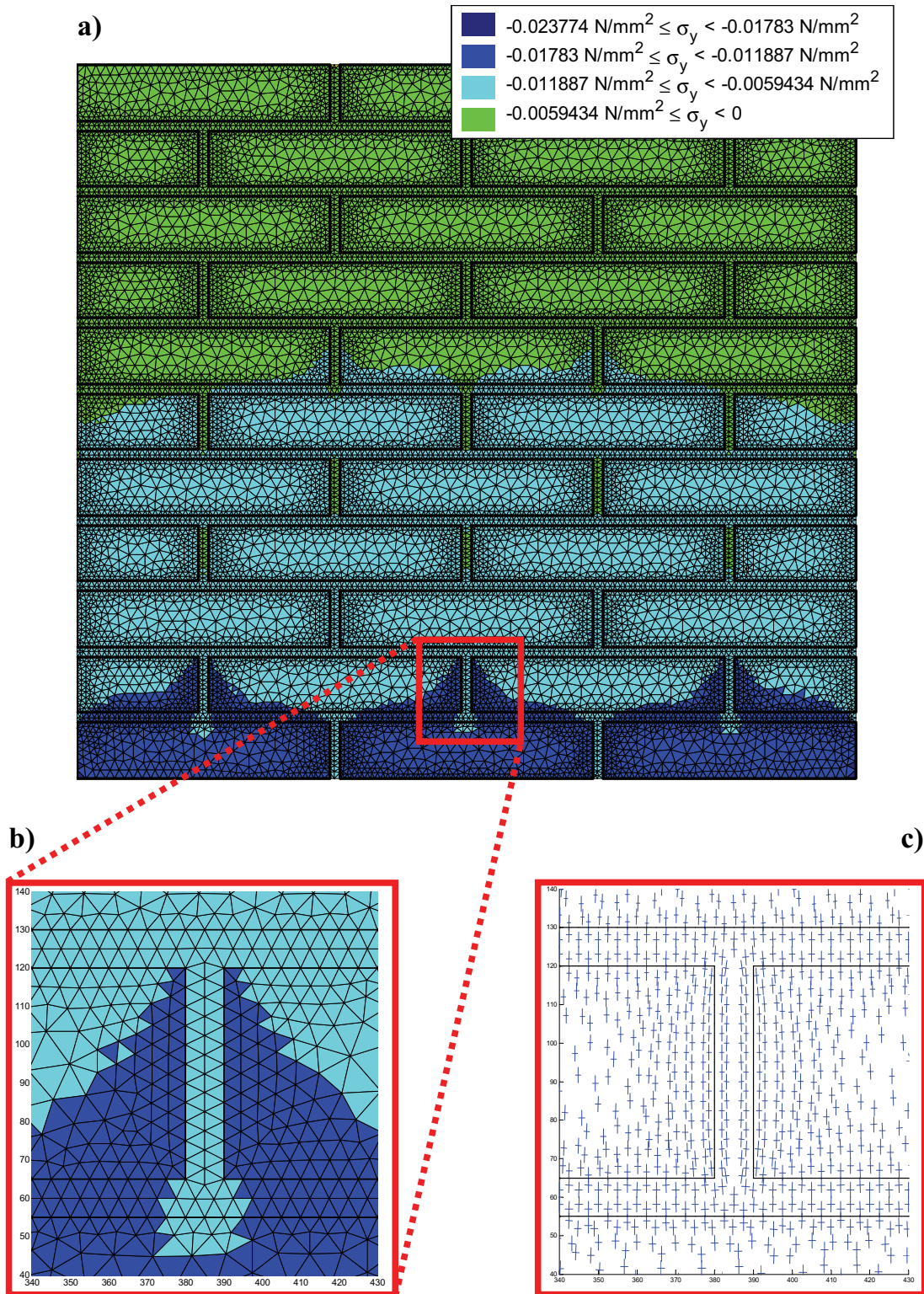


Figure 12: a): Discrete map of the vertical stress. b): Detail of the discrete map of the vertical stress for the boxed area. c): Principal directions of stress for the boxed area.

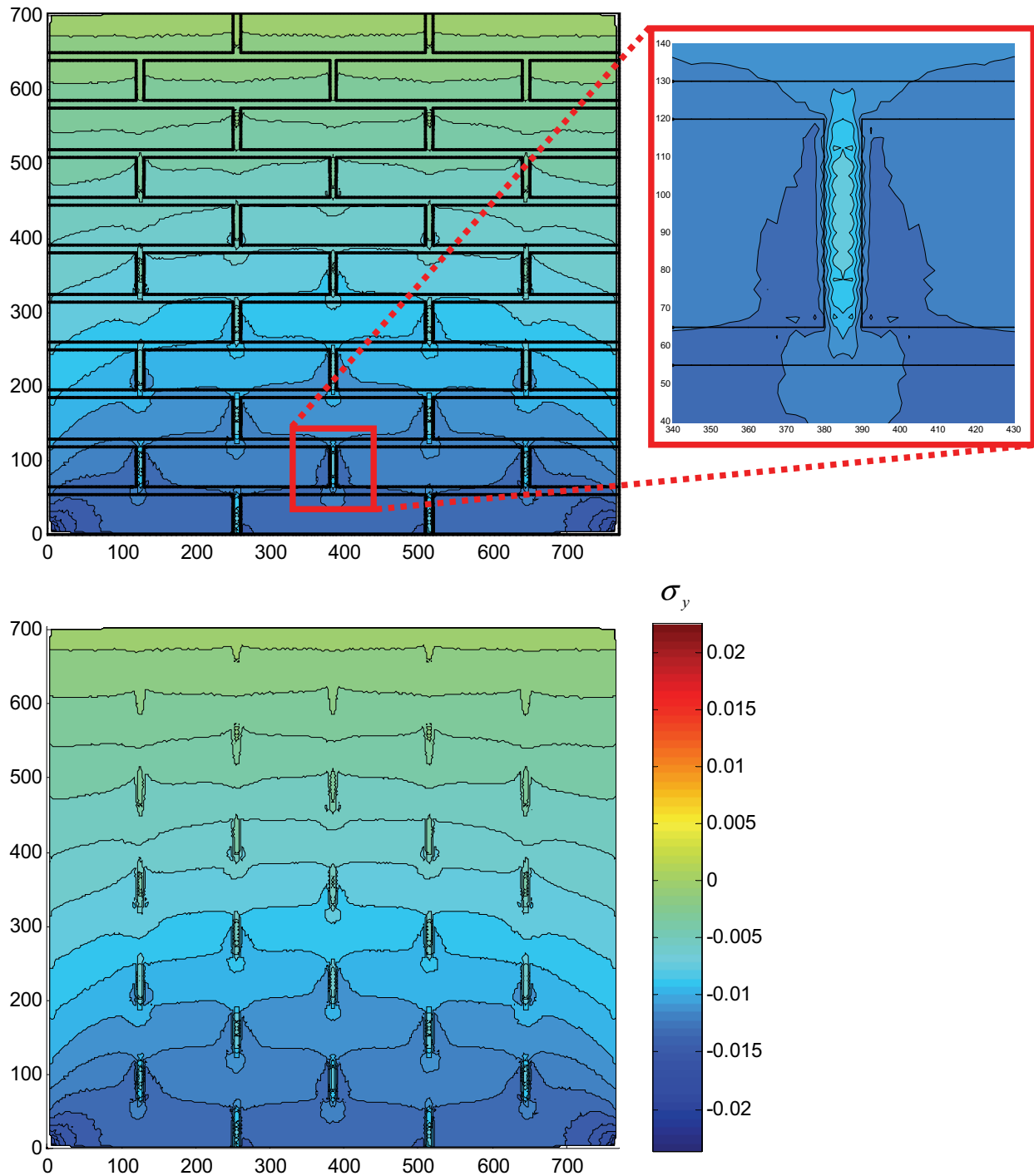


Figure 13: Isolines of the first principal stress, quite similar to the stress along the y axis, with and without superimposition of the masonry lay-up

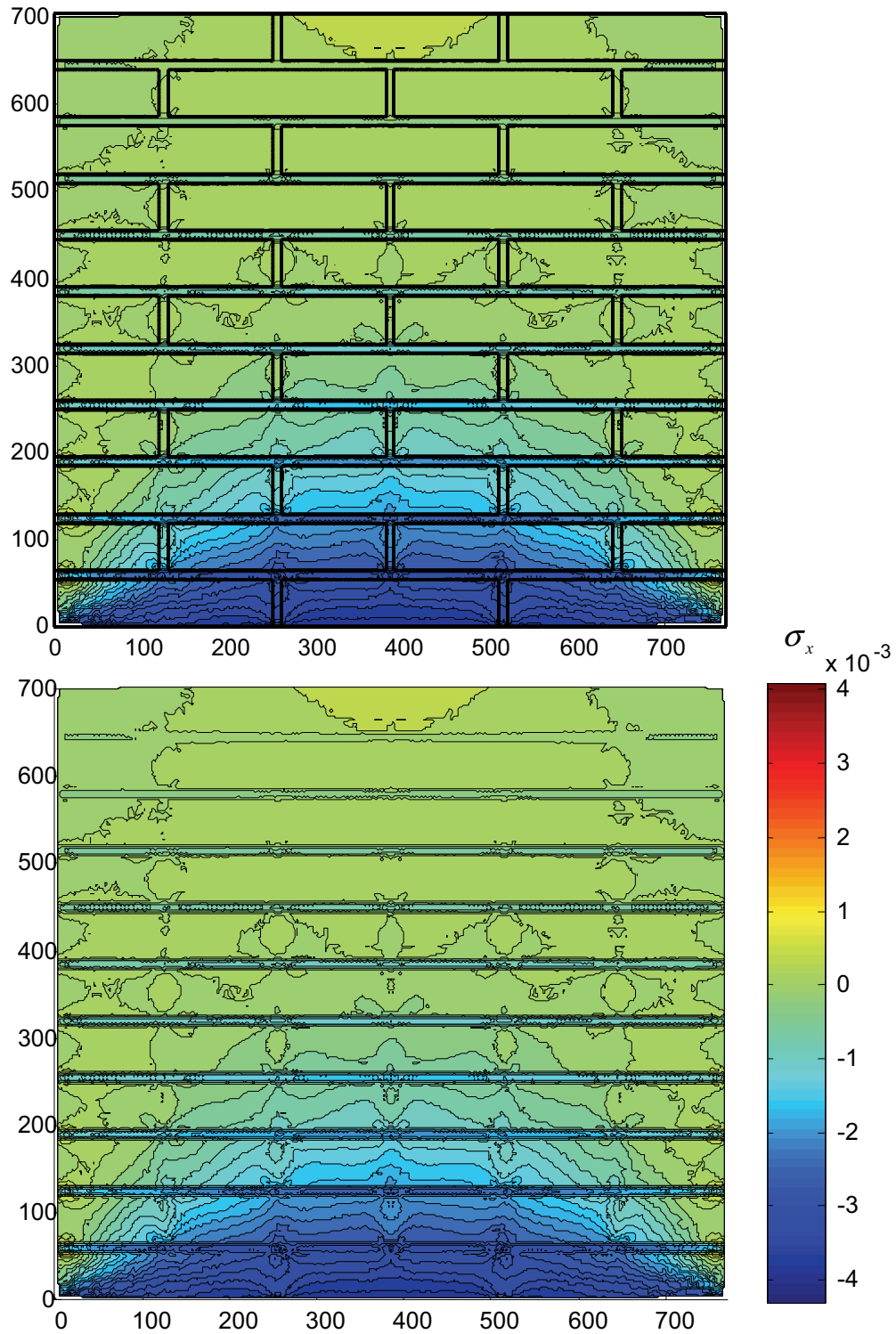


Figure 14: Isolines of the second principal stress, quite similar to the stress along the x axis, with and without superimposition of the masonry lay-up

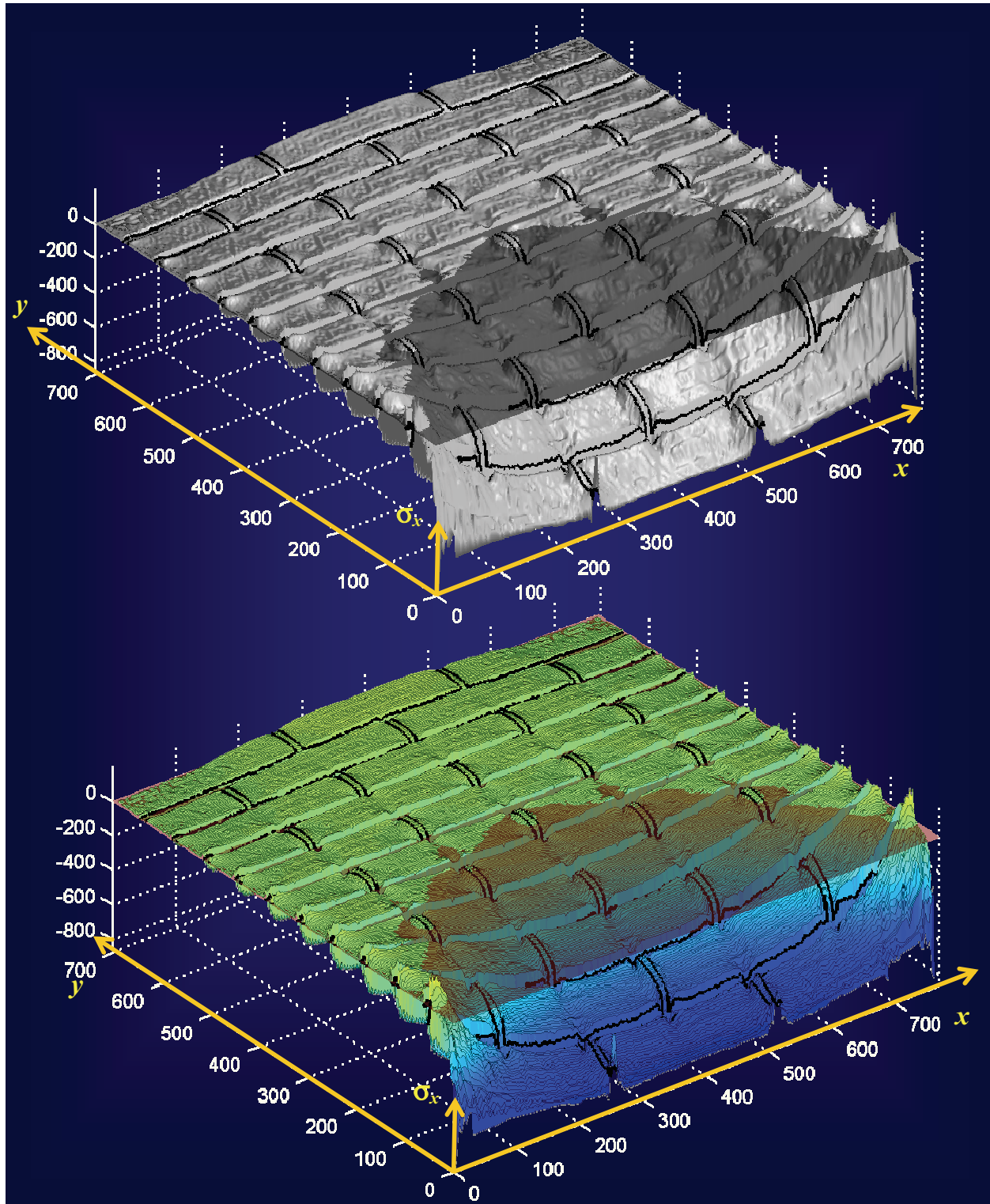


Figure 15: Three-dimensional surface of the stress along the x axis

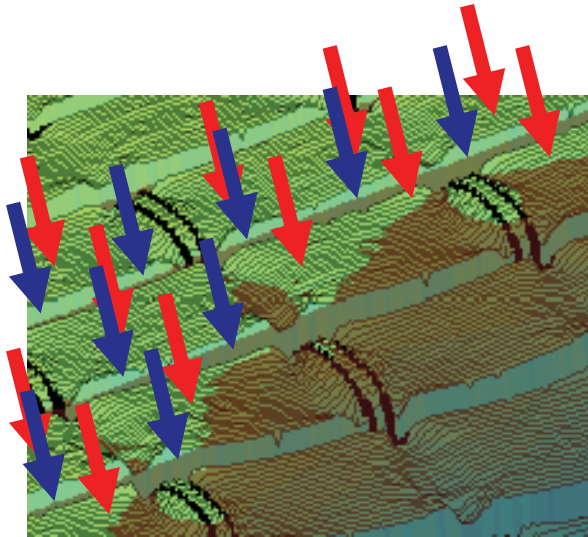


Figure 16: Sign of the stress along the x axis near the neutral axis (detail of Fig. 14)

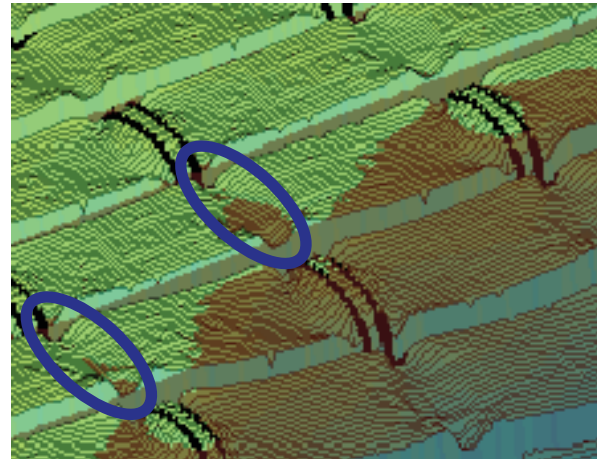


Figure 17: Sign of the stress along the x axis inside the bricks near the neutral axis (detail of Fig. 15)

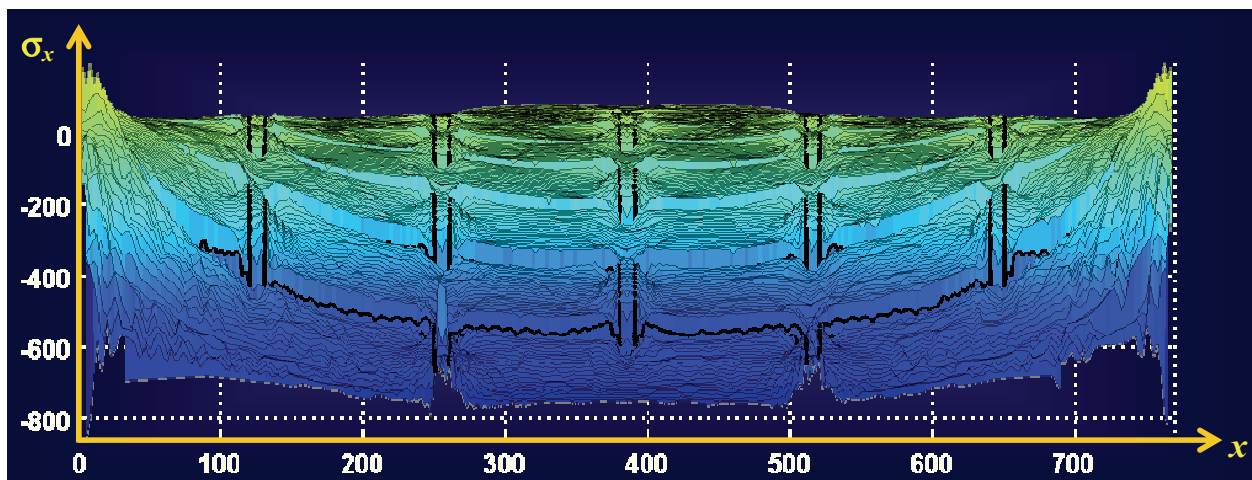


Figure 18: Frontal view of the three-dimensional surface of the stress along the x axis

the central bricks of the first course. Also the three-dimensional surface of the first principal stress (Fig. 19) shows that the mortar is more stressed than the bricks on the horizontal joints and less stressed on the vertical joints.

4 The CM code for modeling crack propagation of masonry walls in shear load

The code we present here preserves the ability to operate in the discrete on domains of several materials, which comes from using the CM, and is characterized by a procedure of re-meshing, acti-

vated by the stress analysis on the Mohr/Coulomb plane. Of the two strategies commonly used for modeling the crack propagation - sharp drop in the normal stress and displacement discontinuity, requiring mesh re-definition (Fig. 20) - we have employed the one describing the crack as a displacement discontinuity, together with a nodal relaxation technique. According to this technique, once the propagation direction has been identified, the crack may be let to propagate either along the mesh side nearest to the computed direction, with an inter-element propagation, or along the

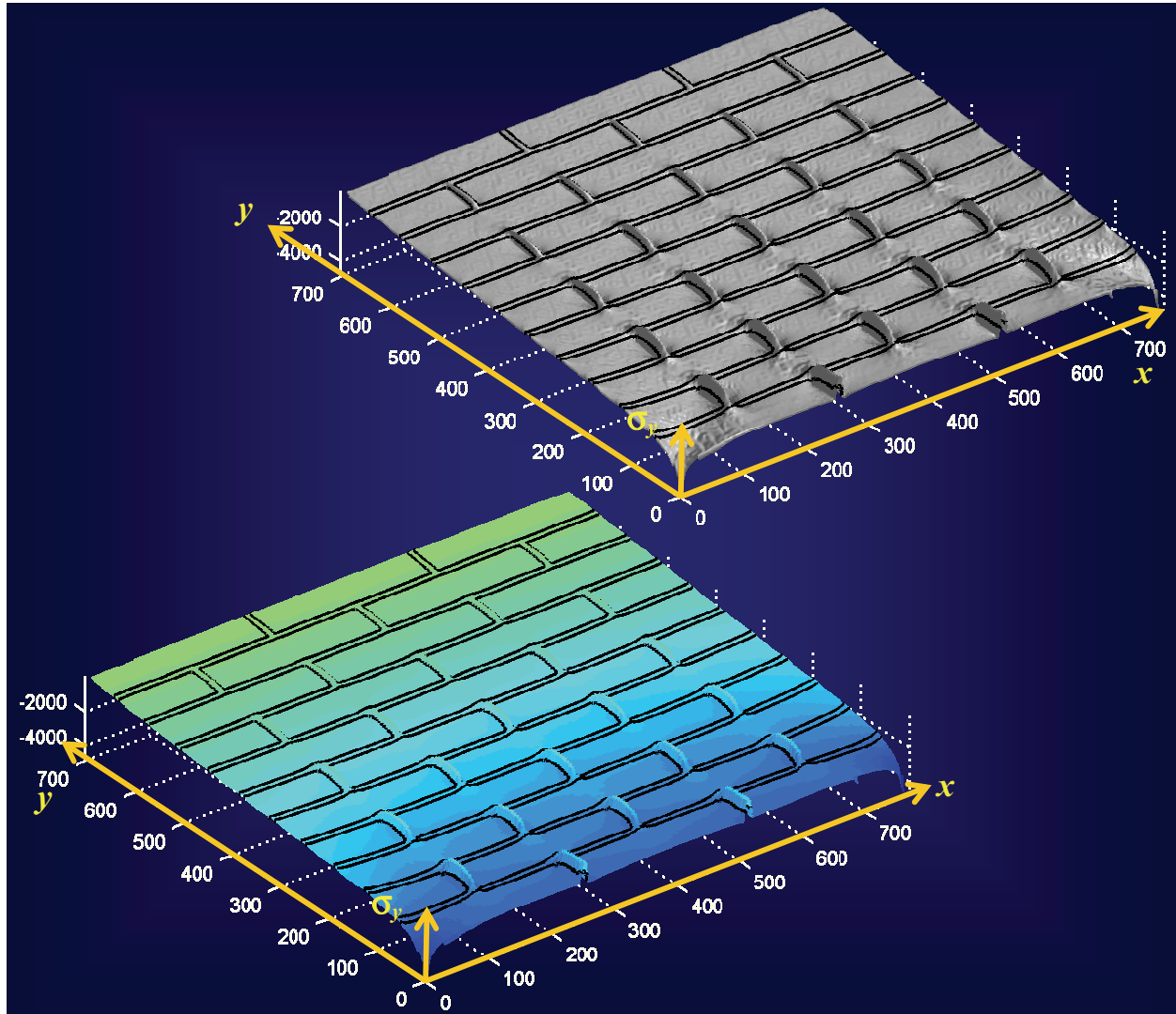


Figure 19: Three-dimensional surface of the stress along the y axis

computed direction, with an intra-element propagation (Fig. 21). In the first case, we need to redefine the inner and outer sides of the mesh. In the second case, we need to update the domain geometry with the new free surfaces and re-generate the mesh. The first technique is faster than the second but is mesh-dependent, while the second is not. Our code uses an intra-element technique.

The stress state on the tip is compared with the Leon criterion in the Mohr/Coulomb plane:

$$\tau_n^2 = \frac{c}{f_c} \left(\frac{f_{tb}}{f_c} + \sigma_n \right). \quad (1)$$

In Eq. 1, c is the cohesion, f_c the compressive strength, and f_{tb} the tensile strength.

The Leon criterion has been adopted both for bricks, mortar and the interfaces, modifying the values of cohesion and angle of internal friction:

	Cohesion (c)	Angle of internal friction (φ)
Mortar	5.238 N/mm^2	10
Brick	11.286 N/mm^2	10
Interface	3 N/mm^2	10

We have then defined a parameter of safeness with respect to the propagation, d , as the minimum distance between the circle of Mohr and the limit curve, with d greater than zero in safeness

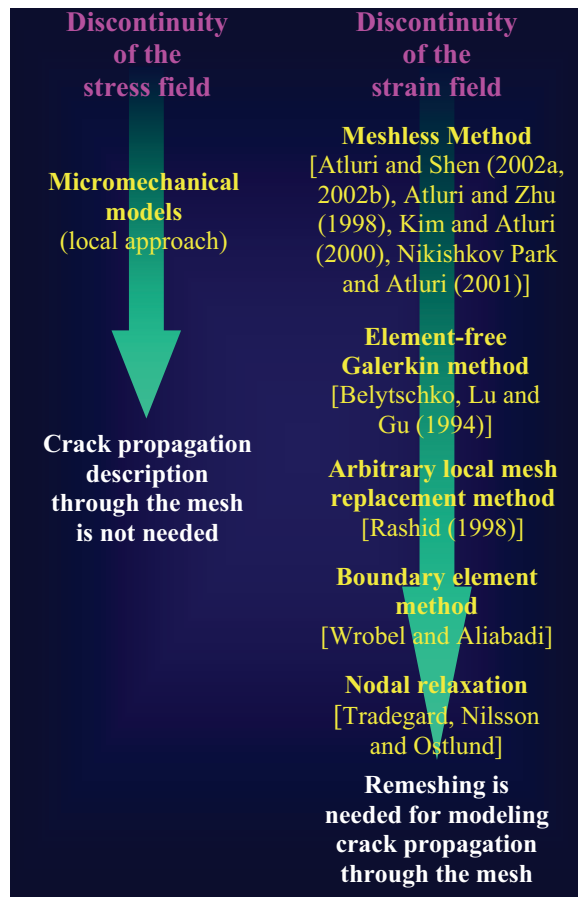


Figure 20: Strategies available to study fracture mechanics using the FEM: sharp drop in the normal stress and displacement discontinuity

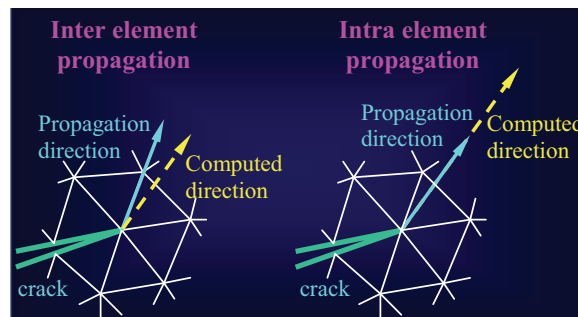


Figure 21: Inter and intra element propagation for the nodal relaxation technique

(Fig. 22) and equal to zero when the crack activates (Fig. 23).

When the circle of Mohr becomes tangent to the Leon curve, the crack activates and the propaga-

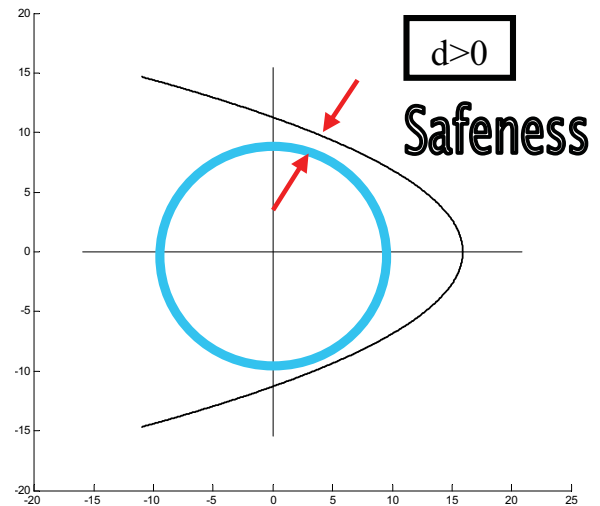


Figure 22: Evaluation of d in safeness conditions

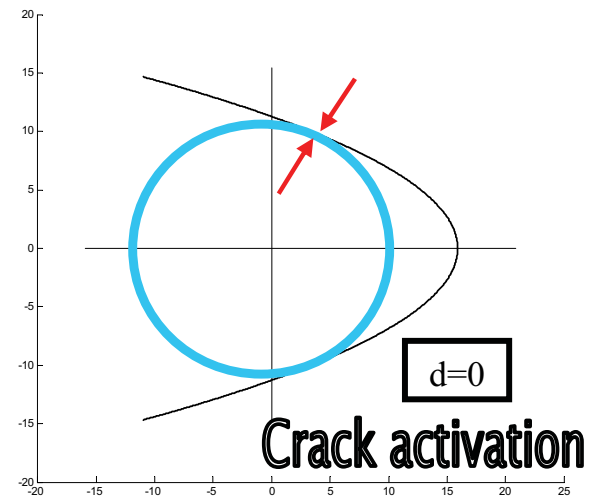


Figure 23: Evaluation of d in limit conditions

tion directions are given by the line joining the pole of Mohr to the two tangent points (Fig. 24). Of the two propagation directions, only one or both activate, depending on the constraint conditions along the directions themselves [Ferretti (2004c)].

The code has been used for simulating a shear test on masonry walls of different boundary conditions and dimensions. The analysis has been carried out in displacement control, leaving the code to identify the initiation points on the two vertical sides of the wall. The code controls the

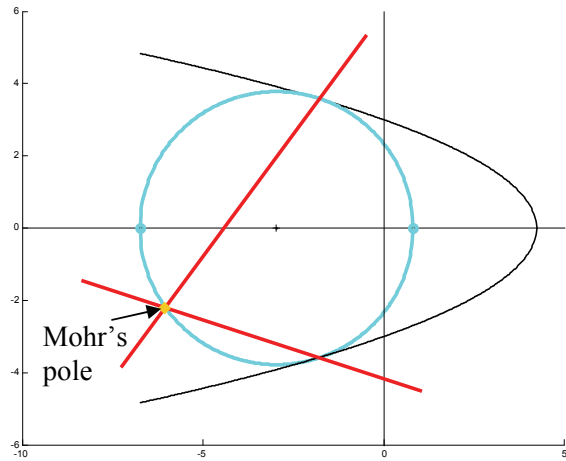


Figure 24: Limit condition and directions of propagation

three-dimensional surface of the safeness parameter for the points of the two vertical sides of the wall (Figs. 25÷27) and identifies a point of initiation whenever the surface intersects the neutral plane of the safeness parameter. For the first value of impressed displacement (Fig. 25), the surface reaches its minimum distance from the neutral plane at the interfaces, for which the safeness parameter is minimum, a medium distance in correspondence of the mortar and its maximum distance in correspondence of the bricks.

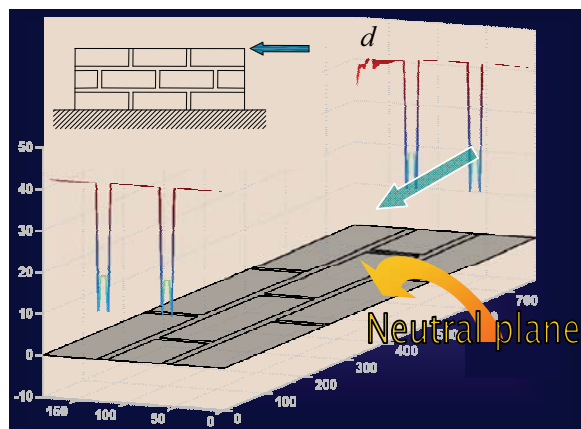


Figure 25: Three-dimensional surface of d on the vertical sides: first value of impressed displacement

For each value of impressed displacement, the

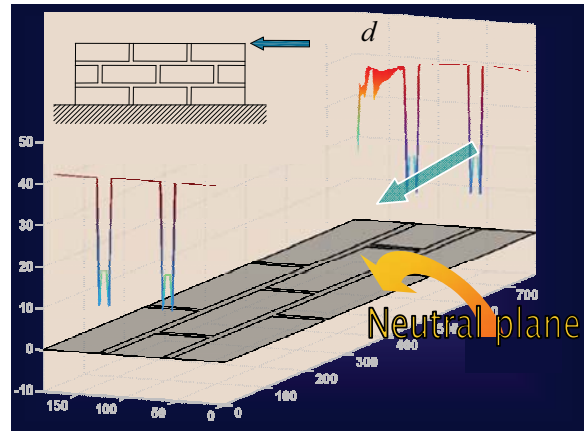


Figure 26: Three-dimensional surface of d on the vertical sides: intermediate value of impressed displacement

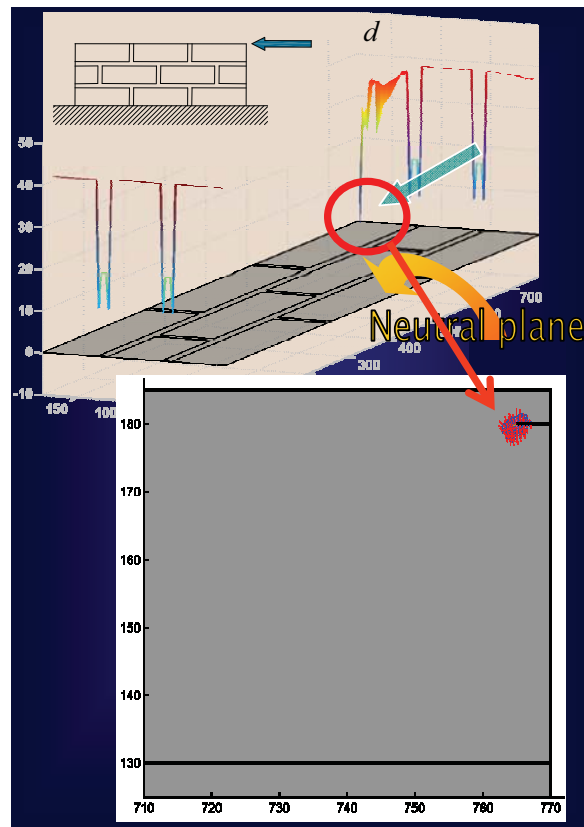


Figure 27: Three-dimensional surface of d on the vertical sides: impressed displacement of crack initiation

code evaluates the parameter d on the two vertical sides of the wall (Fig. 31). If d is greater than

zero, the impressed displacement is increased and the parameter d is re-evaluated for the points of the two vertical sides (Fig. 31 when no crack has initiated).

As we can see in Fig. 26, for a subsequent increases of displacement, the surface of the parameter d modifies in the neighborhood of the point in which the displacement is impressed, stating that in this zone the safeness parameter is decreasing with the increase of impressed displacement. The safeness parameter for the neighborhood of the point of impressed displacement continues to decrease until the surface intersects the neutral plane of the safeness parameter (Fig. 27). At this point, the parameter d is no more greater than zero, and the code updates the domain by adding the two new surfaces where the surface has intersected the neutral plane (detail in Fig. 27). Then, the code performs a static analysis on the tip of the inserted crack (the detail in Fig. 27 shows the principal directions of stress at the tip), in order to evaluate whether or not the crack is propagating (Fig. 31). If not, the impressed displacement is increased, while, if the crack is propagating, the domain is updated once more (Fig. 31), evaluating the propagation directions in the Mohr/Coulomb plane.

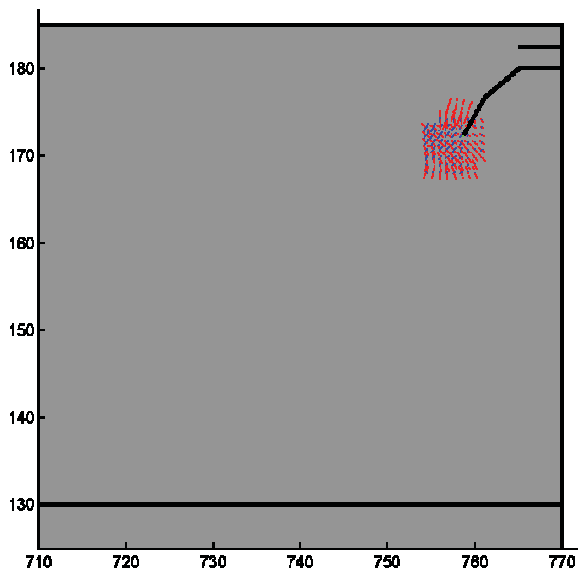


Figure 28: Crack paths for the impressed displacement of first initiation

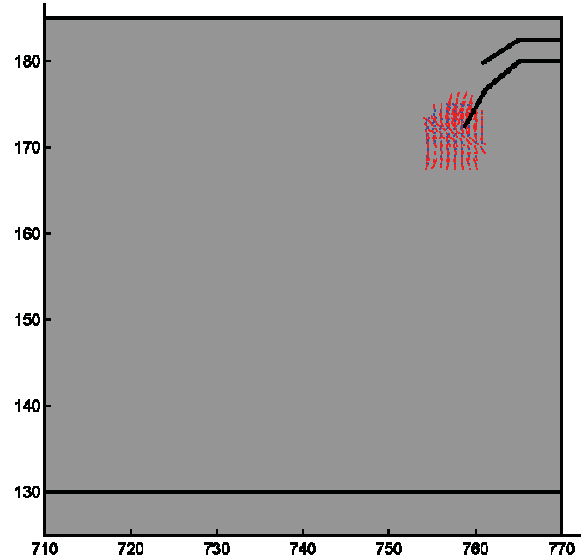


Figure 29: Principal directions of stress at the tip of the first crack after two propagation of the second crack

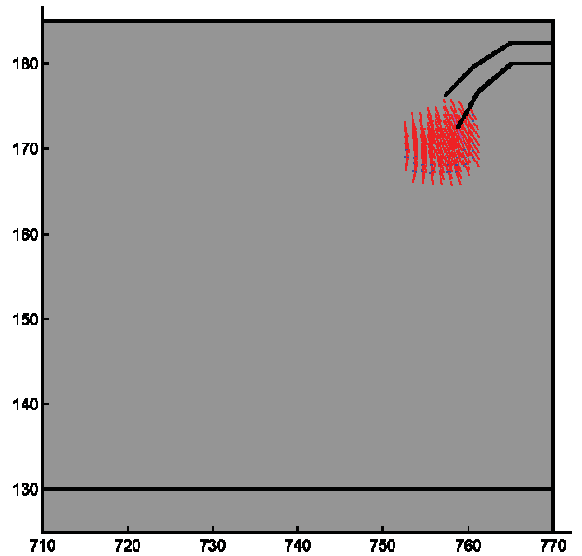


Figure 30: Principal directions of stress at the tip of the first crack after three propagation of the second crack

It is worth noting that the Mohr/Coulomb limit condition always identifies two propagation directions, that is, always identifies crack branching. Nevertheless, the difference between the two propagation directions identified is often negligible. Our code estimates that actually a crack

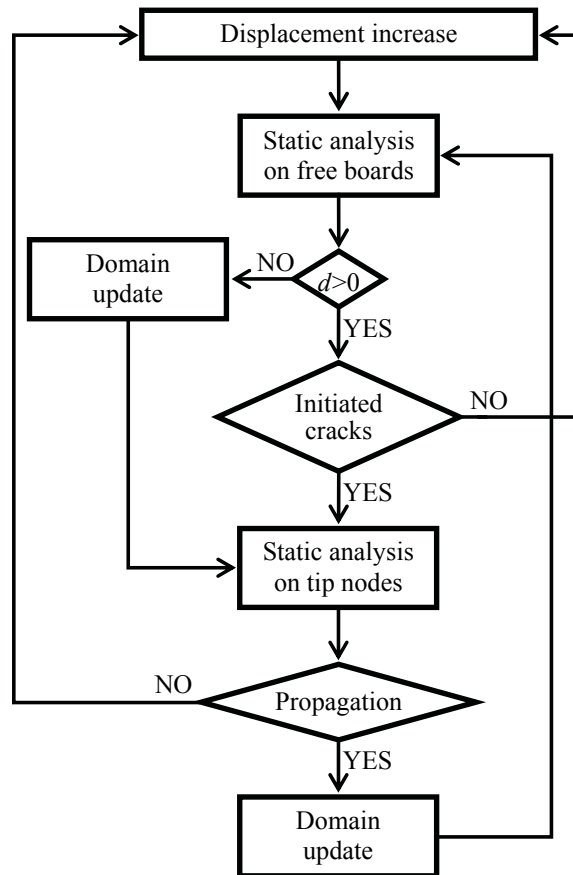


Figure 31: Flow chart of the CM code

branching only occurs if the difference between the two identified propagation directions is greater than a prefixed value, of around 5° . When the crack is let to bifurcate, the uploading procedure of the domain geometry is modified in order to split the new crack tip into two crack tips. Moreover, the crack is let to bifurcate only when the crack tip lies in a brick (crack branching in the mortar or in the interfaces are not taken into account).

Contemporarily to the static analysis on the tip of the inserted crack, the code also performs a static analysis on the two vertical sides, looking for new initiation points. The Fig. 28 shows that, for the value of impressed displacement of first activation, the first crack propagates twice and a second crack initiates just above the first crack.

The code continues to evaluate the stress field on the new tips and on the two vertical sides, until

all the crack stabilizes and there are no more initiation points. Only at this point, is the impressed displacement increased once again (Fig. 31).

We can see how sensitive the code is to the interactions between two propagating cracks, by comparing the principal directions at the tip of the first crack (Fig. 29) with the principal directions at the same tip after one propagation of the second crack (Fig. 30): the principal directions of stress have changed and the tensile state of stress has increased.

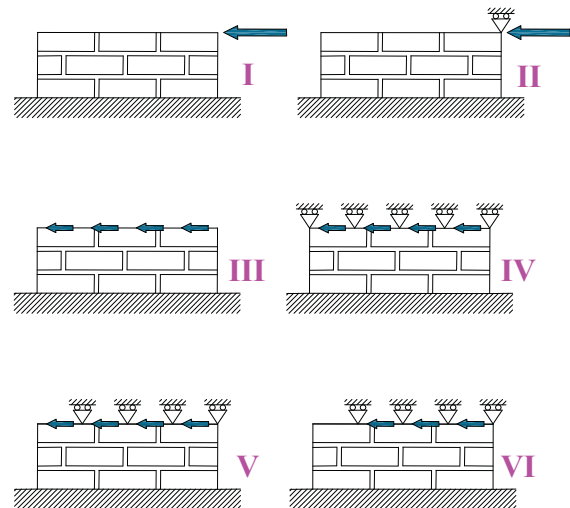


Figure 32: Analyzed boundary conditions

4.1 Stress analysis for different boundary conditions

In Fig. 32, we have six different ways for impressing the displacement to the specimen, simulating six different experimental lay-ups. In the first, the horizontal displacement is impressed only on the upper right corner, which is able to move vertically. In the second, the horizontal displacement is impressed on the upper right corner once more, but the vertical displacement of the upper right corner is constrained. In the third, the horizontal displacement is impressed on each node of the upper side, with free vertical displacements. The fourth is analogous to the third, but the vertical displacement on the upper side is now constrained. The fifth and the sixth are analogous to the fourth, but they take into account the fact that

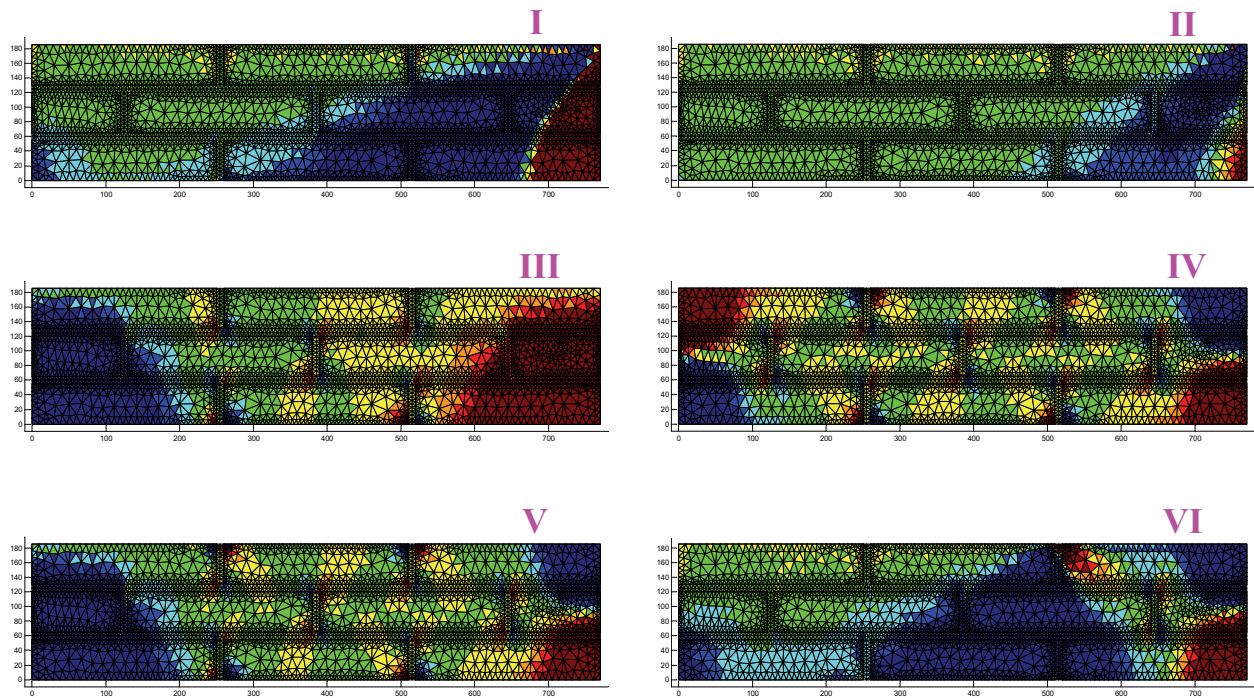


Figure 33: Vertical stresses for the six boundary conditions

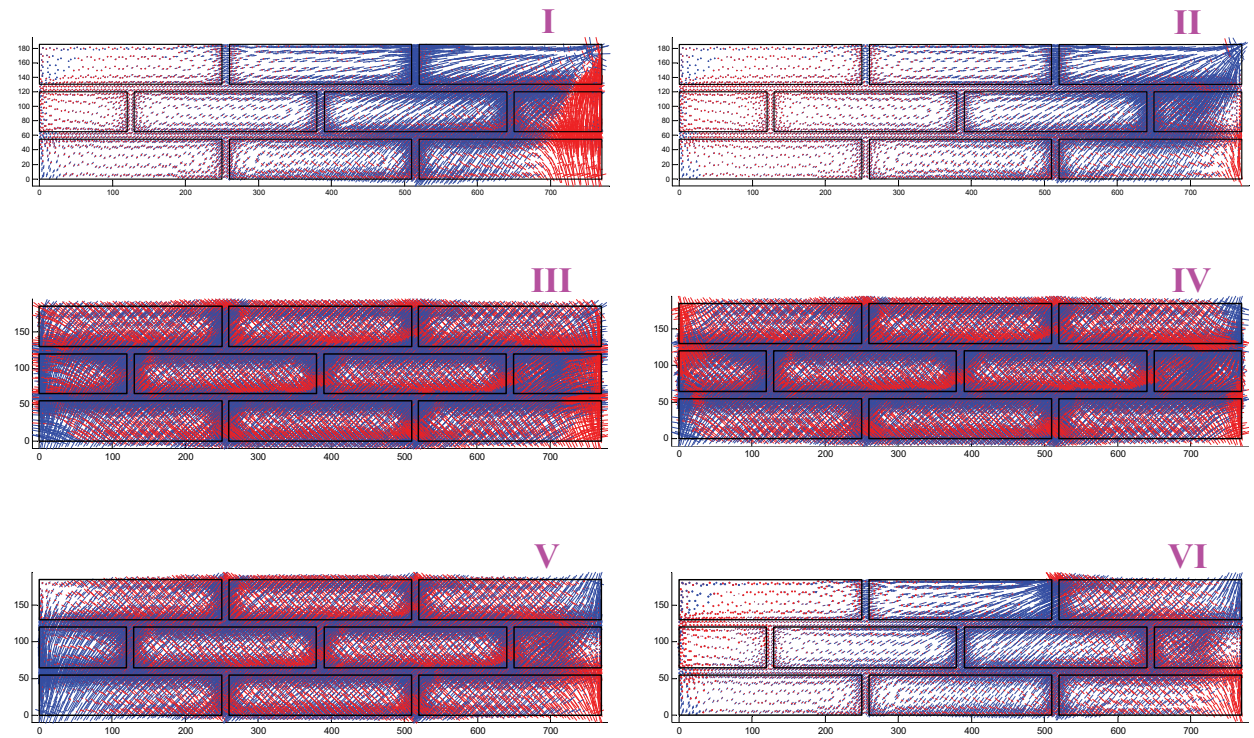


Figure 34: Principal directions of stress for the six boundary conditions

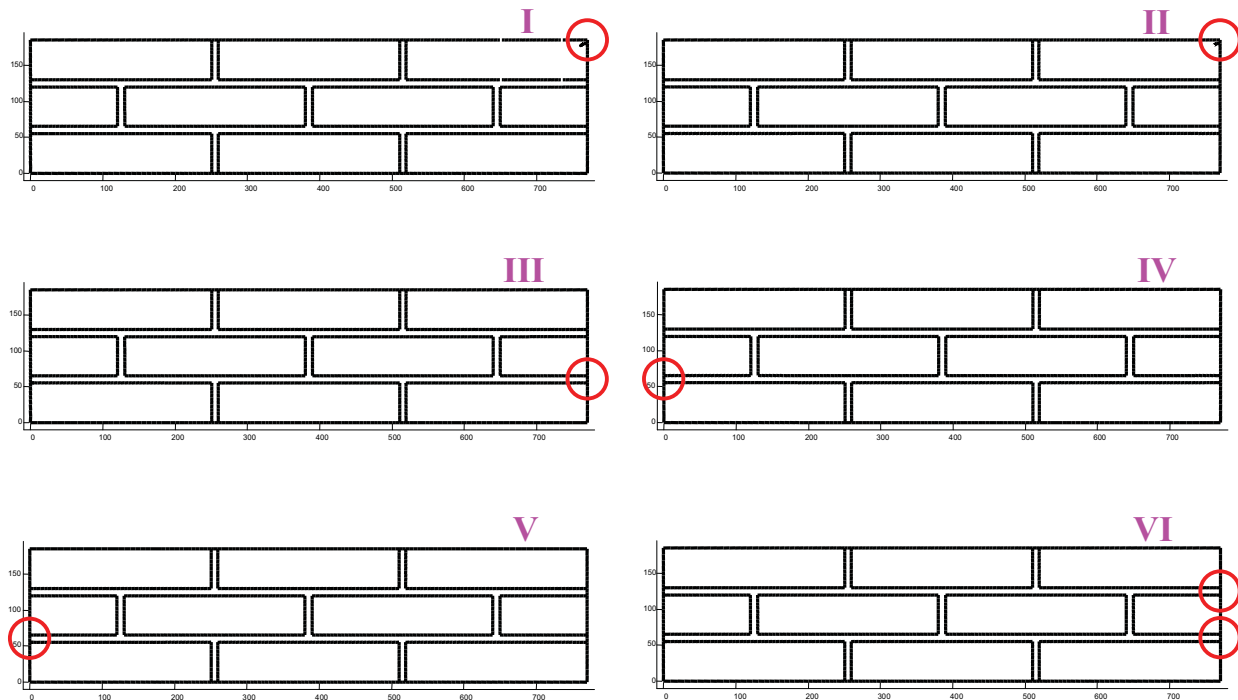


Figure 35: Initiation points for the six boundary conditions: schemes I and II fail in the upper right brick, while schemes III, IV, V, and VI fail in the interfaces between brick and mortar

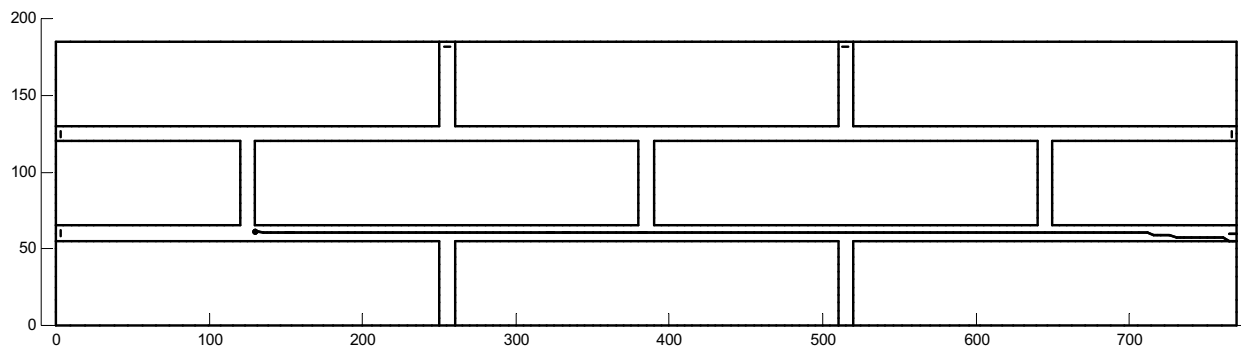


Figure 36: Crack path for the third boundary condition

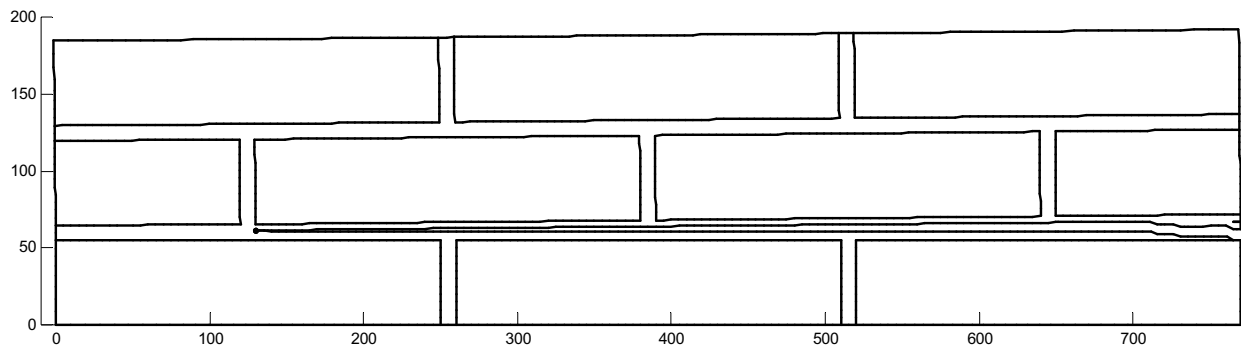


Figure 37: Deformed configuration for the third boundary condition

the bond between testing machine and specimen is unilateral and is able to work only in compression. For this reason, the testing machine is not able to constrain the node vertically on the left of the upper side, since these nodes should be constrained in tension. In the fifth scheme, the testing machine impresses the horizontal displacement onto the relaxed nodes, while it does not do so in the sixth scheme. The number of nodes to unbound is evaluated by the code in function of the impressed displacement.

The Fig. 33 shows the map of the vertical stresses for each scheme of Fig. 32. Of special interest is the comparison between the fourth and the sixth schemes, in the sense that the fourth is the scheme we would realize in laboratory for simulating the masonry answer to a seismic load, while the sixth is the scheme we can actually realize, due to the limits of the bond between the testing machine and the specimen. The stress distribution is quite different in the two cases, and this fact should call our attention to the way in which we have to treat the experimental data when we perform this type of tests.

In Figs. 34 and 35, we have the principal directions of stress and the initiation points for the six schemes, these too being strongly dependent on the way to impress the displacement.

Fig. 36 provides the complete crack path for the third scheme. At it can be seen from the picture, the crack path for this scheme does not feature any crack branching since it always propagates into the mortar. The deformed configuration and the load/displacement diagram for the third scheme are shown in Figs. 37 and 38, respectively. The rotation of the upper side, allowed by the boundary conditions, is clearly evident in Fig. 37.

4.2 Stress analysis for different number of courses

The Fig. 39 shows the stress distribution provided by the CM code for the fourth boundary scheme with three base bricks and three courses, five courses, seven courses, nine courses, and eleven courses of bricks. The stress concentration at the corner of the bricks is clearly evident. The stresses of tension and compression which alter-

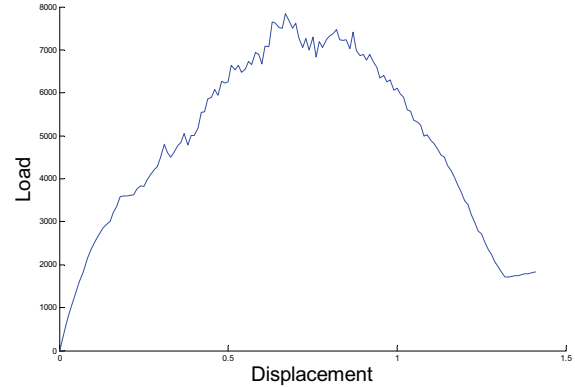


Figure 38: Load/displacement diagram for the third boundary condition

nate at the corners are due to the tendency of the bricks to rotate inside the mortar matrix. We can appreciate the same from the stress maps with continuous coloring, with alternate tension and compression stresses (Fig. 40).

Moreover, we can see how the stress transfer scheme evolves towards the compressed rod scheme as the wall assumes square dimensions. Also the relationship between the stress distribution and the masonry lay-up is well evident in the square wall.

4.3 Crack propagation for the first boundary condition

In this section, we present how the CM code works for the first boundary condition with three courses and three bricks of base.

The code identifies the propagation of three cracks in the upper right brick, one crack in the upper right joint and one crack in the bottom right joint (Fig. 41).

The first crack to enucleate is in the brick (Fig. 42). Then we have propagation of the first crack and initiation and propagation of a second and a third crack in the brick (Fig. 42). When the crack in the upper joint also initiates, the three cracks in the brick stop propagating (Fig. 42). The crack in the upper joint propagates for a while through the mortar, then it reaches and follows the interface and, finally, it penetrates the bottom brick (Fig. 42).

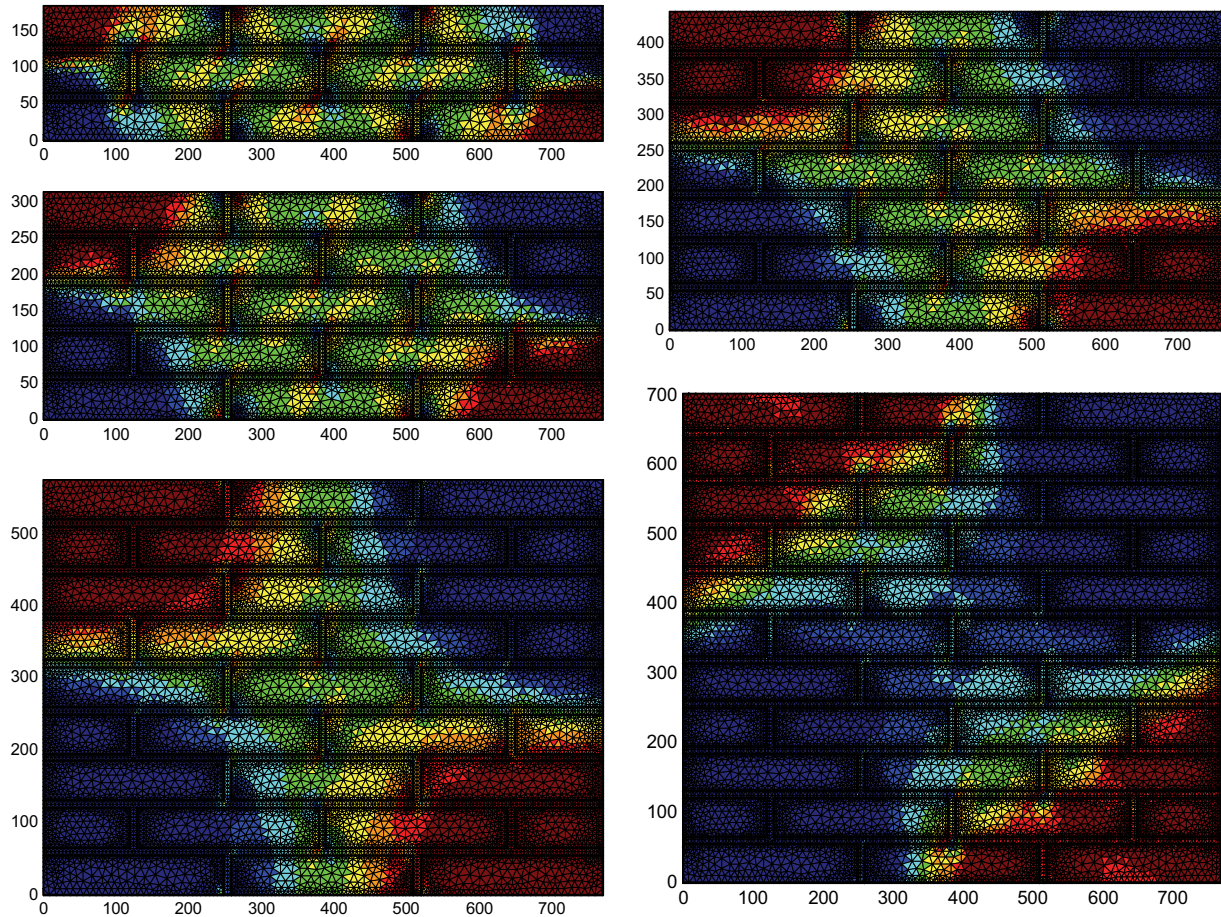


Figure 39: Discrete maps of the vertical stress for the fourth boundary condition and variable number of courses

From this moment forth, this crack does not propagate any more, and the only active crack is the one in the bottom joint (Fig. 42). The detail of the final deformed configuration is shown in Fig. 43.

As it can be seen from Figs. 41–43, for this boundary condition all the cracks propagate without bifurcating, even if some of them lie in a brick.

4.4 Crack propagation for the second boundary condition

In order to compare the propagation paths for unconstrained and constrained vertical displacement on the same scheme, let us now consider the second boundary condition. The propagation differs sensitively in the two cases: when the vertical displacements are constrained, all the initiation points are in the upper right brick and the propagation paths feature several bifurcations,

due to the punching effect of the vertical constraint (Fig. 44).

5 Conclusions

The CM modeling is a micro-modeling which provides us with an accurate two-material analysis, able to show interaction effects between mortar and bricks and stress concentration effects at the corners of the bricks.

The computational capabilities of the CM code have been improved considerably, if compared with those presented in previous studies. In particular, the code is now able to self-estimate the position of crack initiation, which no longer requires definition by the operator. Moreover, the code is able to self-estimate how many cracks initiate, and to manage several cracks propagat-

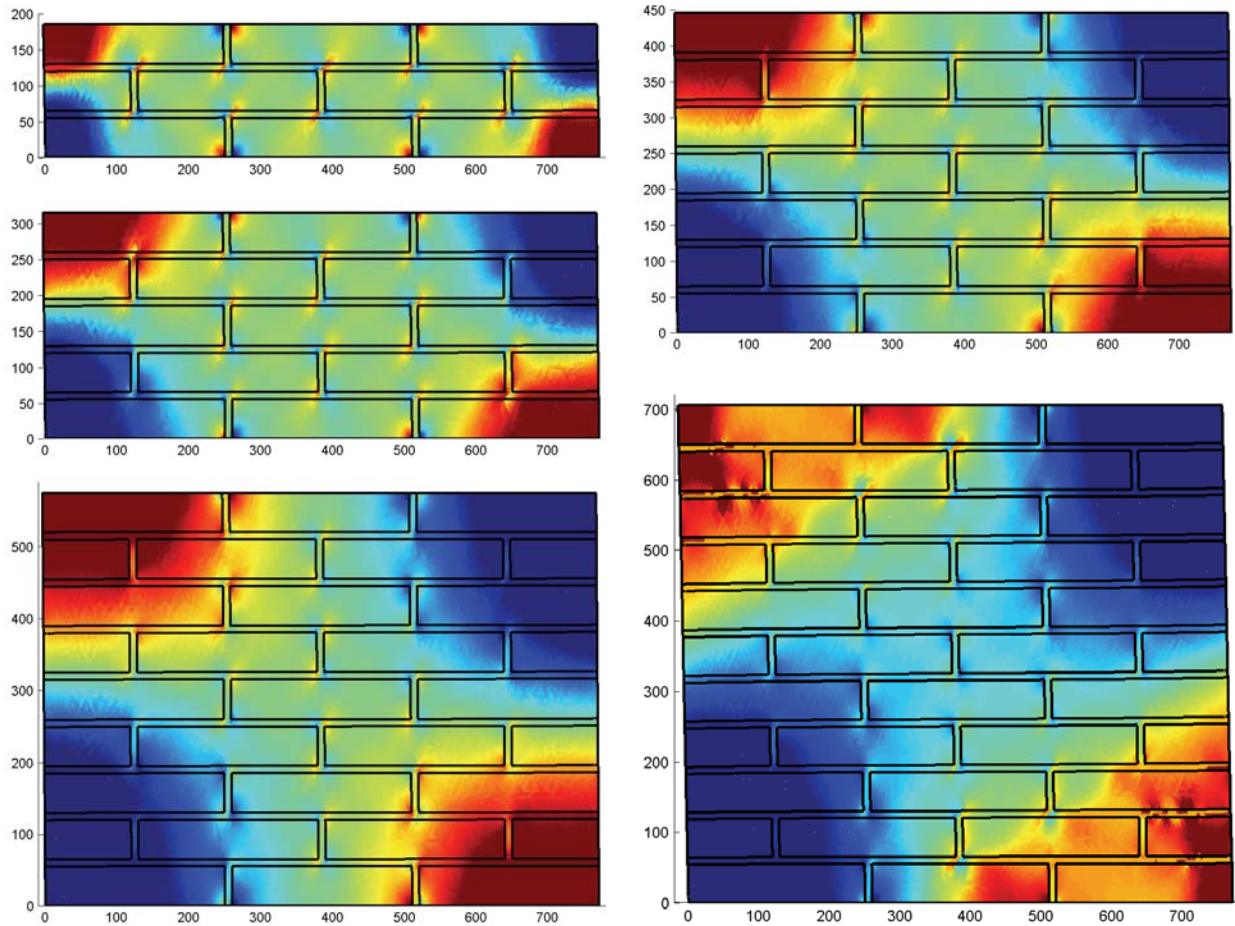


Figure 40: Continuous maps of the vertical stress and deformed configurations for the fourth boundary condition and variable number of courses

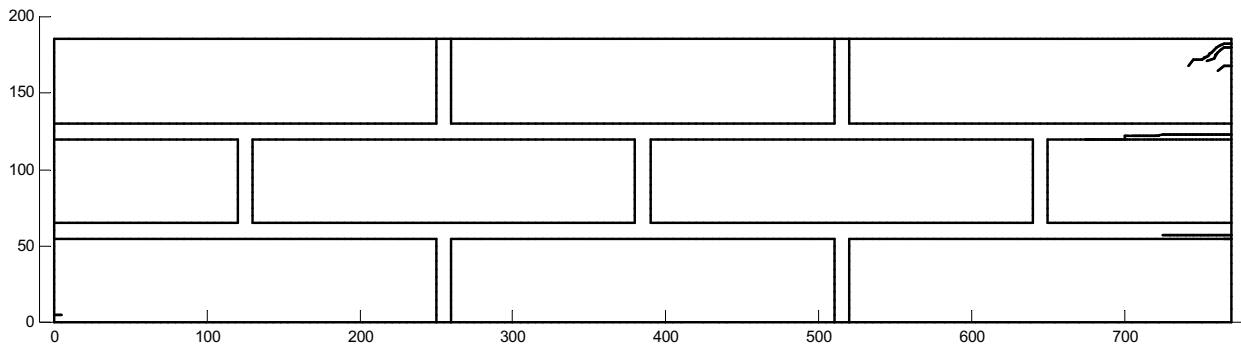


Figure 41: Complete crack path for the first boundary condition with three courses and three bricks of base

ing at the same time. The code is also able to self-estimate whether or not one or more cracks bifurcate and to follow the propagation of each branch of bifurcation. This last peculiarity of the code is particularly remarkable, since, to the authors' knowledge, it is the first time that CM is

used for simulating dynamic crack branching. It is worth noting how the use of CM with automatic re-meshing allows us to overcome some typical unresolved difficulties pointed out in FEM numerical simulations of dynamic crack propagation [Guo and Nairn (2006)] and bifurcation [Abra-

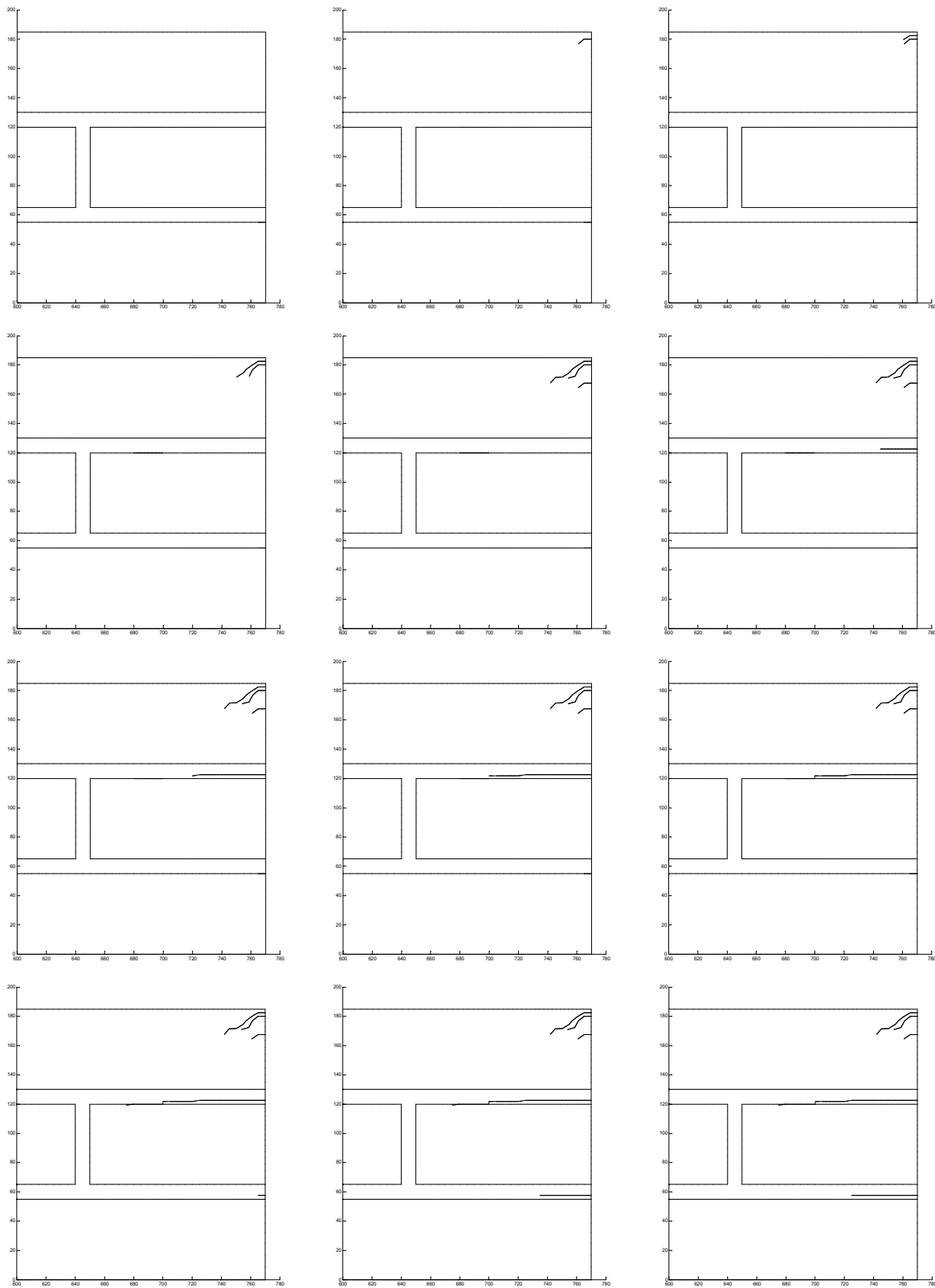


Figure 42: Subsequent steps of crack propagation: detail of the upper right corner

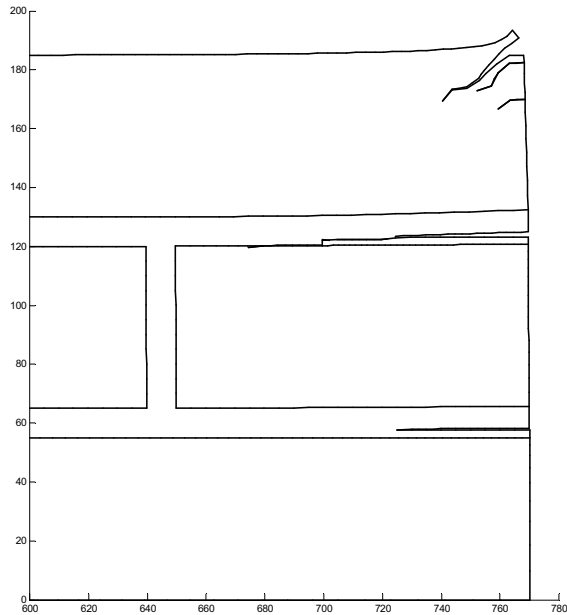


Figure 43: Deformed configuration: upper right corner

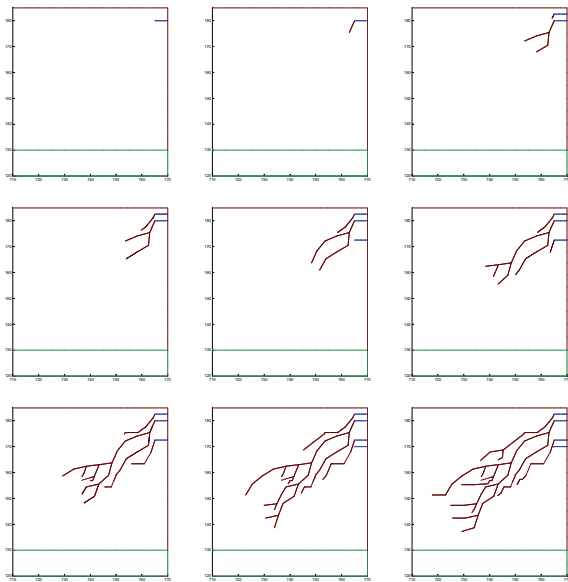


Figure 44: Subsequent steps of crack propagation: detail of the upper right corner

ham (2000), Chen Hu and Chen (2000), Kim and Atluri (2000), Ching and Batra (2001), Nishioka Furutuka Tchouikov and Fujimoto (2002)], such as moving the singularities at the tips, avoiding the spurious oscillations in models with nodal release technique when a propagating crack bifur-

cate and evaluating fracture parameters such as the dynamic J integral and the dynamic stress intensity factors for the branched short cracks, immediately after the bifurcation.

As a consequence of the ability of the code to manage several cracks propagating at the same time, it is possible to take into account the interactions between the propagating cracks.

Finally, the analysis performed on several boundary conditions provides useful information on how to treat the experimental data.

As possible future developments, we can hope that the accurate analysis provided by the code could be useful for calibrating the parameters of the homogenization techniques and for performing a multi-scale analysis, in which the information at the micro-level is provided by the Cell Method alone.

Acknowledgement: The results presented here are part of the CIMEST Scientific Research on the Identification of Materials and Structures, DISTART, Faculty of Engineering, Alma Mater Studiorum, Bologna (Italy). The authors acknowledge the support of the research project PRIN 2006 – Guidelines for the survey and management of historical structures and infrastructures, national coordinator Prof. A. De Stefano, local coordinator Prof. A. Di Leo.

References

- Aboudi, J.** (1991): *Mechanics of Composite Materials*. Elsevier.
- Abraham, F.F.** (2000): MAADLY Spanning the Length Scales in Dynamic Fracture. *CMES: Computer Modeling in Engineering & Sciences*, vol. 1, no. 4, pp. 63-70.
- Alpa, G.; Monetto, I.** (1994): Microstructural Model for Dry Block Masonry Walls with In-plane Loading. *Journal of the Mechanics and Physics of Solids*, vol. 47, no. 7, pp. 1159-1175.
- Anthoine, A.** (1995): Derivation of the In-plane Elastic Characteristics of Masonry through Homogenization Theory. *Int. J. Solids Structures*, vol. 32, no. 2, pp. 137-163.

- Atluri, S.N.; Shen, S.** (2002a): *The Meshless Local Petrov-Galerkin Method*, Tech Science Press.
- Atluri, S.N.; Shen, S.** (2002b): The Meshless Local Petrov-Galerkin (MLPG) Method: A Simple & Less-costly Alternative to the Finite Element and Boundary Element Methods. *CMES: Computer Modeling in Engineering & Sciences*, vol. 3, no. 1, pp. 11-52.
- Atluri, S.N.; Zhu, T.** (1998): A New Meshless Local Petrov-Galerkin (MLPG) Approach in Computational Mechanics. *Comput Mech*, vol. 22, pp. 117-127.
- Belytschko, T.; Lu, Y.Y.; Gu, L.** (1994): Element Free Galerkin Methods. *Int J Num Meth Engrg*, vol. 37, pp. 229-256.
- Bensoussan, A.; Lions, J.L.; Papanicolaou, G.** (1978): *Asymptotic Analysis for Periodic Structures*. North-Holland, Amsterdam.
- Berto, L.; Saetta, A.; Scotta, R.; Vitaliani, R.** (2002): An Orthotropic Damage Model for Masonry Structures. *International Journal for Numerical Methods in Engineering*, vol. 55, no. 22, pp. 127-157.
- Bettini, P.; Trevisan, F.** (2003): Electrostatic Analysis for Plane Problems with Finite-formulation. *IEEE Trans. on Magnetics*, vol. 39, no. 3.
- Carvelli, V.; Maier, G.; Taliercio, A.** (2000): Kinematic Limit Analysis of Periodic Heterogeneous Media. *CMES: Computer Modeling in Engineering & Sciences*, vol. 1, no. 2, pp. 19-30.
- Cecchi, A.; Di Marco, R.** (2000): Homogenization of Masonry Walls with a Numerical Oriented Procedure. Rigid or Elastic Blocks? *Eur. J. Mech., A/Solids*, vol. 19, pp. 535-546.
- Cecchi, A.; Milani, G.; Tralli, A.** (2004): In-plane Loaded CFRP Reinforced Masonry Walls: Mechanical Characteristics by Homogenization Procedures. *Composite Science and Technology*, vol. 64, pp. 2097-2112.
- Cecchi, A.; Rizzi, N.L.** (2001): Heterogeneous Elastic Solids: a Mixed Homogenization-Rigidification Technique. *International Journal of Solids and Structures*, vol. 38, pp. 29-36.
- Cecchi, A.; Sab, K.** (2002): A Multi-parameter Homogenization Study for Modelling Elastic Masonry. *Eur. J. Mech. A/Solids*, vol. 21, pp. 249-268.
- Chen, Z.; Hu, W.; Chen, E.P.** (2000): Simulation of Dynamic Failure Evolution in Brittle Solids without Using Nonlocal Terms in the Strain-Stress Space. *CMES: Computer Modeling in Engineering & Sciences*, vol. 1, no. 4, pp. 57-62.
- Ching, H.K.; Batra, R.C.** (2001): Determination of Crack Tip Fields in Linear Elastostatics by the Meshless Local Petrov-Galerkin (MLPG) Method. *CMES: Computer Modeling in Engineering & Sciences*, vol. 2, no. 2, pp. 273-290.
- Chiostrini, S.; Vignoli, A.** (1989): Application of a Numerical Method to the Study of Masonry Panels with Various Geometry under Seismic Loads. In *Structural Repair and Maintenance of Historical Buildings (Edited by C. A. Brebbia)*, Computational Mechanics Publications.
- Como, M.; Grimaldi, A.** (1985): A Unilateral Model for Limit Analysis of Masonry Walls. *II Meeting on Unilateral Problems in Structural Analysis, CISM Courses and Lectures*, Springer Verlag, vol. 288, pp. 223-238.
- Cosmi, F.** (2005): Elastodynamics with the Cell Method. *CMES: Computer Modeling in Engineering & Sciences*, vol. 8, no. 3, pp. 191-200.
- de Buhan, P.; de Felice, G.** (1997): A Homogenization Approach to the Ultimate Strength of Brick Masonry. *Journal of the Mechanics and Physics of Solids*, vol. 45, no. 7, pp. 1085-1104.
- de Felice, G.** (1995): Détermination des Coefficients d'Élasticité de la Maçonnerie par une Méthode d'Homogénéisation. In *Actes du 12ème Congrès Français de Mécanique*, Strasbourg, vol. 1, pp. 393-396.
- Del Piero, G.** (1989): Constitutive Equations and Compatibility of the External Loads for Linear Elastic Masonry-like Materials. *Meccanica*, vol. 24, pp. 150-162.
- Del Piero, G.** (1998): Limit Analysis and Nontension Materials. *Int. J. Plasticity*, vol. 14, pp. 259-271.
- Di Pasquale, S.** (1992): New Trends in the Anal-

ysis of Masonry Structures. *Meccanica*, vol. 27, pp. 173-184.

Duvaut, G. (1984): Homogénéisation et Matériaux Composites. In *Trends and Applications of Pure Mathematics to Mechanics (Edited by P. G. Ciarlet and M. Roseau)*, Lecture Notes in Physics, Springer-Verlag, Berlin, vol. 195, pp. 35-62.

Ferretti, E. (2001): *Modellazione del Comportamento del Cilindro Fasciato in Compressione*, Ph.D. Thesis (in Italian), University of Lecce, Italy.

Ferretti, E. (2003): Crack Propagation Modeling by Remeshing using the Cell Method (CM). *CMES: Computer Modeling in Engineering & Sciences*, vol. 4, no. 1, pp. 51-72.

Ferretti, E. (2004a): A Cell Method (CM) Code for Modeling the Pullout Test Step-wise. *CMES: Computer Modeling in Engineering & Sciences*, vol. 6, no. 5, pp. 453-476.

Ferretti, E. (2004b): Experimental Procedure for Verifying Strain-Softening in Concrete. *Int. J. Fracture* (Letters section), vol. 126, no. 2, pp. L27-L34.

Ferretti, E. (2004c): Crack-Path Analysis for Brittle and Non-brittle Cracks: a Cell Method Approach. *CMES: Computer Modeling in Engineering & Sciences*, vol. 6, no. 3, pp. 227-244.

Ferretti, E. (2005): A Local Strictly Nondecreasing Material Law for Modeling Softening and Size-Effect: a Discrete Approach. *CMES: Computer Modeling in Engineering & Sciences*, vol. 9, no. 1, pp. 19-48.

Ferretti, E.; Di Leo, A. (2003): Modelling of Compressive Tests on FRP Wrapped Concrete Cylinders through a Novel Triaxial Concrete Constitutive Law. *SITA*, vol. 5, pp. 20-43.

Ferris, M.; Tin-Loi, F. (2001): Limit Analysis of Frictional Blocks Assemblies as a Mathematical Problem with Complementary Constraints. *Int. J. Mech Sci.* vol. 43, pp. 209-224.

Formica, G.; Sansalone, V.; Casciaro, R. (2002): A Mixed Solution Strategy for the Non-linear Analysis of Brick Masonry Walls. *Comput. Methods Appl. Engrg.*, vol. 191, pp. 5847-5876.

Gambarotta, L.; Lagomarsino, S. (1997): Dam-

age Models for the Seismic Response of Brick Masonry Shear Walls. Part I: the Mortar Joint Model and its Applications. *Earth Eng. Struct. Dyn.*, vol. 26, pp. 423-439.

Gambarotta, L.; Lagomarsino, S. (1997): Damage Models for the Seismic Response of Brick Masonry Shear Walls. Part II: the Continuum Model and its Applications. *Earth Eng. Struct. Dyn.*, vol. 26, pp. 441-462.

Giambanco, G.; Rizzo, S.; Spallino, R. (2001): Numerical Analysis of Masonry Structures via Interface Models. *Comput. Methods Appl. Mech. Eng.*, vol. 190, pp. 6493-6511.

Giaquinta, M.; Giusti, E. (1985): Researches on the Equilibrium of Masonry Structures. *Arch. Rat. Mech. Anal.*, vol. 88, pp. 359-392.

Grimaldi, A.; Luciano, R.; Sacco, E. (1992): Nonlinear Dynamic Analysis of Masonry Structures via FEM. In *Computing Methods in Applied Science and Engineering (Edited by R. Glowinski)*, Nova Science Publishers, pp. 373-382.

Guo, Y.J.; Nairn, J.A. (2006): Three-Dimensional Dynamic Fracture Analysis Using the Material Point Method. *CMES: Computer Modeling in Engineering & Sciences*, vol. 16, no. 3, pp. 141-155.

Heshmatzadeh, M.; Bridges, G.E. (2007): A Geometrical Comparison between Cell Method and Finite Element Method in Electrostatic. *CMES: Computer Modeling in Engineering & Sciences*, vol. 18, no. 1, pp. 45-58.

Heyman, J. (1966): The Stone Skeleton. *Int. J. Solids and Structures*, vol. 2, pp. 249-279.

Lofti, H.R.; Benson Shing, P. (1994): Interface Model Applied to Fracture of Masonry Structures. *J. Struct. Eng., ASCE*, vol. 120, no. 1, pp. 63-80.

Lourenço, P.B. (1995): *An Orthotropic Continuum Model for the Analysis of Masonry Structures*. Report 03.21.1.31.27, University of Delft, Delft, Holland.

Lourenço, P.B. (1996): *Computational Strategies for Masonry Structures*. Ph.D. Thesis, Delft University of Technology, Delft, The Netherlands.

Lourenço, P.B.; de Borst, R.; Rots, J.G. (1997): A Plane Stress Softening Plasticity Model for Or-

thotropic Materials. *International Journal for Numerical Methods in Engineering*, vol. 40, pp. 4033-4057.

Lourenço, P.B.; Rots, J.G. (1997): A Multi-surface Interface Model for the Analysis of Masonry Structures. *J. Eng. Mech., ASCE*, vol. 123, no. 7, pp. 660-668.

Luciano, R.; Sacco, E. (1997): Homogenization Technique and Damage Model for Old Masonry Material. *Int. J. Solids Structures*, vol. 34, no. 24, pp. 3191-3208.

Luciano, R.; Sacco, E. (1998): A Damage Model for Masonry Structures. *Eur. J. Mech., A/Solids*, vol. 17, no. 2, pp. 285-303.

Kim, H. G.; Atluri, S. N. (2000) Arbitrary Placements of Secondary Nodes, and Error Control, in the Meshless Local Petrov-Galerkin (MLPG) Method. *CMES*, vol. 1, no. 3, pp. 11-32.

Kralj, B.; Pande, G.N.; Middleton, J. (1991): On the Mechanics of Frost Damage to Brick Masonry. *Comp & Struct.*, vol. 41, pp. 53-66.

Lee, S.J.; Pande, G.N.; Kralj, B. (1998): A Comparative Study on the Approximate Analysis of Masonry Structures. *Materials and Structures*, vol. 31, no. 211, pp. 473-479.

Marrone, M.; Mitra, R. (2004): A Theoretical Study of the Stability Criteria for Generalized FDTD Algorithms for Multiscale Analysis. *IEEE Trans. on Antennas and Propagation*, vol. 52, no. 8.

Marrone, Grassi, P.; M.; Mitra, R. (2004): A New Technique Based on the Cell Method for Calculation the Propagation Constant of Inhomogeneous Filled Waveguide. *IEEE Trans. on Antennas and Propagation*.

Maier, G.; Nappi, A.; Papa, E. (1991): On Damage and Failure of Brick Masonry. In *Experimental and Numerical Methods in Earthquake Engineering* (Donea, Jones, P.M. Eds.), Ispra, pp. 223-245.

Masiani, R.; Rizzi, N.; Trovalusci, P. (1995): Masonry Walls as Structured Continua. *Meccanica*, vol. 30, pp. 673-683.

Massart, T.J. (2003): *Multi-Scale Modeling of Damage in Masonry Structures*. Ph.D. Thesis.

University of Bruxelles.

Milani, G. (2004): *Homogenization Techniques for In- and Out-of-plane Loaded Masonry Walls*. Ph.D Thesis. Graduate School in Civil and Industrial Engineering, University of Ferrara, Italy, Department of Engineering.

Mura, T. (1987): *Micromechanics of Defects in Solids*. Martinus Nijhoff Publishers.

Nikishkov, G. P.; Park, J. H.; Atluri, S. N. (2001): SGBEM-FEM Alternating Method for Analysing 3D Non-planar Cracks and Their Growth in Structural Components. *CMES: Computer Modeling in Engineering & Sciences*, vol. 2, no. 3, pp. 401-422.

Nishioka, T.; Furutuka, J.; Tchouikov, S.; Fujimoto, T. (2002): Generation-Phase Simulation of Dynamic Crack Bifurcation Phenomenon Using Moving Finite Element Method Based on Delaunay Automatic Triangulation. *CMES: Computer Modeling in Engineering & Sciences*, vol. 3, no. 1, pp. 129-145.

Pande, G.N.; Liang, J.X.; Middleton, J. (1989): Equivalent Elastic Moduli for Brick Masonry. *Comp. Geotech.*, vol. 8, pp. 243-265.

Pegon. P.; Anthoine, A. (1997): Numerical Strategies for Solving Continuum Damage Problems with Softening: Application to the Homogenisation of Masonry. *Computers and Structures*, vol. 64, no. 1-4, pp. 623-642.

Pietruszczak, S.; Niu, X. (1992): A Mathematical Description of Macroscopic Behaviour of Brick Masonry. *Int. J. Solids Structures*, vol. 5, no. 29, pp. 531-546.

Rashid, M.M. (1998): The Arbitrary Local Mesh Replacement Method: an Alternative to Remeshing for Crack Propagation Analysis. *Comput Methods Appl Mech Engrg*, vol. 154, pp. 133-150.

Romano, G.; Romano, M. (1979): Sulla Soluzione di Problemi Strutturali in Presenza di Legami Costitutivi Unilateri. *Atti Acc. Naz. Linc. Serie VIII, LXVII*.

Romano, G.; Sacco, E. (1987): Convex Problems in Structural Analysis. In *Unilateral Problems in Structural Analysis*, (Edited by G. Del

Piero and F. Maceri), *CISM Courses and Lectures*, Springer Verlag, vol. 304, pp. 279-297.

Sanchez-Palencia, E. (1987): Non Homogeneous Media and Vibration Theory. *Lecture Notes in Physics*, Springer-Verlag, Berlin, vol. 127.

Shrive, N.G.; England, G.L. (1991): Elastic Creep and Shrinkage Behaviour of Masonry. *Int. J. Solids Structures*, vol. 29, pp. 103-109.

Specogna, R.; Trevisan, F. (2005): Discrete Constitutive Equations in A- χ Geometric Eddy-Current Formulation. *IEEE Trans. on Magnetics*, vol. 41, no. 4.

Straface, S.; Troisi, S.; Gagliardi, V. (2006): Application of the Cell Method to the Simulation of Unsaturated Flow. *CMC: Computers, Materials and Continua*, vol. 3, no. 3, pp. 155-166.

Tonti, E. (2001a): A Direct Discrete Formulation of Field Laws: the Cell Method. *CMES: Computer Modeling in Engineering & Sciences*, vol. 2, no. 2, pp. 237-258.

Tonti, E. (2001b): A Direct Discrete Formulation for the Wave Equation. *Journal of Computational Acoustics*, vol. 9, no. 4, pp. 1355-1382.

Tradegard, A.; Nilsson F.; Ostlund S. (1998): FEM-Remeshing Technique Applied to Crack Growth Problems. *Comput Method Appl M*, vol. 160, pp. 115-131.

Trevisan, F.; Kettunen, L. (2004): Geometric Interpretation of Discrete Approaches to Solving Magnetostatics. *IEEE Trans. on Magnetics*, vol. 40, no. 2.

Wrobel, L.C.; Aliabadi, M.H. (2002): *The Boundary Element Method*, Wiley-Vch.

Zucchini A.; Lourenço, P.B. (2002): A Micro-Mechanical Model for the Homogenisation of Masonry. *Int. J. Solids Structures*, vol. 39, pp. 3233-3255.

